Plasma cells identified as the most abundant gluten peptide-MHC expressing cells in celiac disease gut lesions

Short title: Plasma cells as antigen presenting cells

Lene Støkken Høydahl[1,2,*], Lisa Richter[3,4], Rahel Frick[1,2], Omri Snir[1], Kristin Støen Gunnarsen[1,2], Ole JB Landsverk[3], Rasmus Iversen[1], Jeliazko R Jeliazkov[5], Jeffrey J Gray[5,6,7], Elin Bergseng[1], Stian Foss[1,2], Shuo-Wang Qiao[1,8], Knut EA Lundin[1,9], Jørgen Jahnsen[10,11], Frode L Jahnsen[3], Inger Sandlie[1,2], Ludvig M Sollid[1,8] & Geir Åge Løset[1,2,12*]

[1]*Centre for Immune Regulation and Department of Immunology, University of Oslo and Oslo University Hospital, Oslo, Norway.*

[2]*Centre for Immune Regulation and Department of Biosciences, University of Oslo, Oslo, Norway.*

[3]*Centre for Immune Regulation and Department of Pathology, University of Oslo and Oslo University Hospital, Oslo, Norway.*

[4]*Present address: Core Facility Flow Cytometry, Biomedical Center Munich, Ludwig-Maximilians-Universität Munich, Planegg-Martinsried, Germany*

[5]*Program in Molecular Biophysics, Johns Hopkins University, Baltimore, Maryland, USA.*

[6]*Department of Chemical and Biomolecular Engineering and Institute of NanoBioTechnology, Johns Hopkins University, Baltimore, Maryland, USA.*

[7]*Sidney Kimmel Comprehensive Cancer Center, Johns Hopkins School of Medicine, Baltimore, Maryland, USA.*

[8]*KG Jebsen Coeliac Disease Research Centre and Department of Immunology, University of Oslo, Oslo, Norway.*

[9]*Department of Gastroenterology, Oslo University Hospital-Rikshospitalet Oslo, Norway.*

[10]*Department of Gastroenterology, Akershus University Hospital, Lørenskog, Norway.*

[11]*Institute of Clinical Medicine, University of Oslo, Oslo, Norway.*

[12]*Nextera AS, Oslo, Norway.*

Grant support: This work received funding from the South-Eastern Norway Regional Health Authority (grant 2012046) and by the Research Council of Norway through its Centers of Excellence funding scheme, project number 179573/V40. JRJ and JJG are supported by the U.S. National Institutes of Health grant R01-GM078221. Part of the computations were performed on resources provided by UNINETT Sigma2 - the National Infrastructure for High Performance Computing and Data Storage in Norway. We would like to thank Sivaganesh Sathiaruby, Linn Margrethe Eggesbø and Anna Bujko for

excellent technical assistance, Espen Bækkevold for technical advice, Kjetil Taskén (Biotechnology Center of Oslo) for access to the Biacore T100 instrument, The Flow Cytometry Core Facility (FCCF) at Oslo University Hospital for access to equipment and assistance with sorting and the Department of Immunology at Oslo University Hospital-Rikshospitalet for HLA typing.

Abbreviations: APC, antigen presenting cell; BCR, B-cell receptor; CD, celiac disease; DC, dendritic cell; LP, lamina propria; mAb, monoclonal antibody; Mf, macrophage; MHCII, MHC class II; PC, plasma cell; pMHC, peptide-MHC; TG2, transglutaminase 2.

* Correspondence should be addressed to Lene Støkken Høydahl (Address: Department of Immunology, Oslo University Hospital-Rikshospitalet, Sognsvannsveien 20, 0027 Oslo; phone: +47 95033115; fax: +47 23073510; email: l.s.hoydahl@medisin.uio.no) or Geir Åge Løset (Address: Department of Biosciences, University of Oslo; phone: +47 45025421; fax: +47 23073510; email: g.a.loset@ibv.uio.no).

Author contributions: GÅL, IS and LMS conceived the study. LSH, LR, RF, OS, KSG, OJBL, RI, JRJ, EB and SWQ designed, performed experiments and analyzed data. SF provided crucial reagents. JJ and KEAL performed endoscopic examination and provided biopsies. JJG, FLJ, IS, LMS and GÅL designed experiments, analyzed data and supervised the study. LSH, IS, LMS and GÅL wrote the manuscript. All authors critically reviewed the manuscript.

Conflict of interest: LSH, RF, IS, LMS and GÅL are holders of a patent application on the mAbs against gluten-pMHC complexes. The remaining of the authors discloses no conflicts of interest.

Abstract

Background & aims: The pathogenesis of celiac disease (CD) is thought to be driven by a transglutaminase 2 (TG2)-dependent inflammatory $CD4^+$ T-cell response in the gut towards deamidated gluten peptides in the context of disease-associated HLA-DQ molecules. We aimed to gain insight into the antigen presentation process underlying this mucosal immune response.

Methods: We generated monoclonal antibodies (mAbs) specific for the peptide-MHC (pMHC) complex HLA-DQ2.5 and the immunodominant gluten epitope DQ2.5-glia-α1a using phage display. Using these mAbs we assessed gluten peptide presentation in freshly prepared single-cell suspensions of patient intestinal biopsies.

Results: The mAbs allowed specific detection of *in vivo* generated pMHC complexes on the cells of gut biopsies from CD patients consuming gluten. Surprisingly, we identified B cells and plasma cells (PCs) as the most abundant cells presenting DQ2.5-glia-α1a in the inflamed mucosa. Further, we demonstrate that a group of these PCs expresses B-cell receptors (BCRs) specific for either gluten peptides or the autoantigen TG2. MHC class II (MHCII) expression was not restricted to these specific PCs associated with CD, but was observed at an average of 30% of the gut PCs both in CD patients as well as in non-inflamed tissue.

Conclusions: A population of PCs in the gut expresses MHCII and is the most abundant cell type presenting the immunodominant gluten peptide DQ2.5-glia-α1a. These results suggest an important and previously unappreciated role of PCs in the gut as antigen presenting cells (APCs). PCs may thus be responsible for promoting and sustaining intestinal inflammation such as in CD.

Keywords: Antigen presentation; celiac disease; autoimmunity; plasma cells.

Introduction

Gluten-reactive CD4$^+$ T cells are believed to play a key role in celiac disease (CD)[1]. Genetic risk factors, presence of autoantibodies and T-cell mediated destruction of organ-specific cells are shared features between CD and many other autoimmune disorders[1]. However, unlike most of these other conditions, the driving antigen of CD is known, namely dietary gluten proteins from wheat, barley and rye.

The strongest genetic risk factor of CD is HLA, with 90% of the patients expressing HLA-DQ2.5 (*DQA1*05-DQB1*02*), and the vast majority of the remaining patients expressing HLA-DQ8 (*DQA1*03-DQB1*03:02*) or HLA-DQ2.2 (*DQA1*02:01-DQB1*02*)[2]. A consistent finding in HLA-DQ2.5$^+$ CD patients is a CD4$^+$ T-cell response towards the post-translationally modified epitopes DQ2.5-glia-α1a (9mer core region PFPQPELPY) and DQ2.5-glia-α2 (PQPELPYPQ) of α-gliadin, and DQ2.5-glia-ω1 (PFPQPEQPF) and DQ2.5-glia-ω2 (PQPEQPFPW) of ω-gliadin[3,4]. Transglutaminase 2 (TG2)-mediated deamidation of glutamine residues to glutamate introduces negatively charged anchor residues which make the gluten peptides bind more strongly to HLA-DQ2.5, thus increasing the pMHC half-life critical for T-cell engagement[4-6].

Initial activation of mucosal T-cells is thought to take place in gut-draining mesenteric lymph nodes and in gut-associated lymphoid tissue, while re-activation of gut-homing memory/effector T cells primarily occurs in the lamina propria (LP) of the small intestine[1,7]. Previous studies on the characteristics of antigen presenting cells (APC) in the duodenum have identified the macrophages (Mfs) and dendritic cells (DCs) as the main populations[8-10], and a particular CD11c$^+$ population appears to accumulate in active celiac lesions in response to gluten antigen challenge[11]. When DCs and Mfs were isolated from intestinal biopsies of untreated CD patients, loaded with peptide *in vitro* and incubated with gluten-reactive T-cell clones, T-cell activation was indeed observed, the CD11c$^+$ enriched population being most effective[8]. A hallmark of CD is the presence of terminally differentiated plasma cells (PCs) in the LP that are secreting antibodies against deamidated gluten

peptides and TG2[12,13]. However, a pathogenic role of these PCs and the antibodies they secrete have not been established.

To enable specific characterization of the APC subsets involved in gluten peptide presentation, we isolated mAbs with specificity for the DQ2.5-glia-α1a epitope in complex with HLA-DQ2.5 from a naïve, human scFv-phage library. The isolated mAbs discriminate between highly similar pMHC complexes. We further utilized the mAbs to detect both *in vitro* gluten peptide-loading of APCs, and endogenous gluten peptide presentation by cells isolated from intestinal biopsies from CD patients. Surprisingly, B cells and PCs were the main cell types found to present. Our data thus show that PCs, and not DCs and Mfs, is the most abundant cell type that actually presents gluten peptides in the LP of CD patients. Furthermore, the PCs do this by virtue of a hitherto unappreciated ability to express MHCII and present specific antigenic peptides to T cells. This observation may also hold true for other MHCII-associated diseases, and mechanistically explain the beneficial effects seen after B cell depletion therapy even in the absence of pathogenic autoantibodies[14,15].

Material and Methods

Human material

Duodenal biopsy material was obtained according to approved protocols (Regional Ethics Committee of South-Eastern Norway approval 2010/2720 S-97201), and all subjects gave informed written consent. CD diagnosis was given according to the British Society for Gastroenterology guidelines including clinical history, anti-TG2 serological testing, HLA typing and histological analysis of small intestinal biopsies obtained by esophagogastroduodenoscopy and forceps sampling from the duodenum[16]. Small intestinal resections (duodenum-proximal jejunum tissue) were obtained from nonpathological small intestine during Whipple procedure (pancreatoduodenectomy) of pancreatic cancer patients who gave informed written consent (approval 2010/2720 S-97201). Only material with confirmed normal histology was included.

Recombinant pMHC

Recombinant pMHCs are detailed in Supplementary Table 2. Recombinant pMHC used for SPR was purified by size exclusion using Superdex 200 after biotinylation.

Selection and rescue of scFv phage libraries and reformatting and expression of clones

HLA-DQ2.5:DQ2.5-glia-α1a-specific binders were isolated from a naïve human scFv library[17] (obtained from Affitech AS). Selection and rescue was performed essentially as described[18] with the following specifications: pre-blocked phage samples were incubated 1 h with 80 nM biotinylated HLA-DQ2.5:CLIP2 before capture onto Dynabeads MyOne Streptavidin T1 beads for 30 min; unbound phage was transferred to tubes containing 80 nM biotinylated HLA-DQ2.5:DQ2.5-glia-α1a for 1 h before transfer to beads; R4 stringency included 100x less antigen and 20 + 20 washes. Selection alternative 1 was performed as previously described for the OMV selection[18]; alternative 2 included 16.6 nM non-biotinylated HLA-DQ2.5:DQ2.5-glia-α1a as competitor in solution. Phage rescue (*E. coli*

XL1-Blue and M13K07), PEG/NaCl precipitation, spot titration, reformatting and soluble expression was performed as described[18]. scFv's were purified as described[19]. SDS-PAGE was performed using standard procedures.

Binding analysis by SPR and ELISA

SPR was performed using a Biacore T100 (T200 sensitivity enhanced, GE) essentially as described[19]. Samples were 3-fold diluted from 2 µM for single-cycle kinetics experiments and specificity assessments, while 0.25 µM was used for half-life comparisons of scFv and hIgG1 variants. Presence of functionally folded pMHC was verified after running samples by injection of 0.2 µM mAb SPV-L3, binding only correctly folded HLA-DQ2. ELISA was performed as described[18] and detailed in Supplementary Table 3.

IgG cloning, eukaryotic protein expression and purification

hIgG1 cloning was performed as described[18]. Alternatively, synthetic gene fragments encoding V_H and V_L were ordered together with codon optimized mouse Ig gamma2b or mouse Ig kappa cDNA, respectively, and cloned as BsmI-BamHI fragments. HEK293E cells were co-transfected as described[20]. mAbs were purified on either HiTrap protein L (GE) or a NIP-coupled column (in-house prepared) before size exclusion.

Retroviral transduction of A20 murine B cells

A20 B cells expressing HLA-DQ2.5 with the covalently attached DQ2.5-glia-α1a (deamidated=E, native=Q, pL7Q and pY9F variants), DQ2.5-glia-ω1, DQ2.5-glia-α2 as well as HLA-DQ2.5:CLIP2 have been described[19]. The construct encoding HLA-DQ2.5:DQ2.5-glia-α1a-Sα72I was generated by cloning a BglII/BamHI codon-optimized synthetic DNA fragment (Genscript) encoding the HLA-DQ2.5 α-chain (*DQA1*05:01*) with the Sα72I mutation into the pMIG-II-eGFP retroviral plasmid (gift from Dario

Vignali, University of Pittsburgh, Pittsburgh, USA) already encoding HLA-DQ2.5:DQ2.5-glia-α1a[19]. HLA-DQ2.2:DQ2.5-glia-α1a was generated by exchange of the HLA-DQ2.5 α-chain (*DQA1*05:01*) with a BglII/BamHI codon-optimized synthetic DNA fragment encoding the HLA-DQ2.2 α-chain (*DQA1*02:01*). Cells were transduced and stained for flow cytometric analysis as described[19] (Supplementary Table 4).

Differentiation and flow cytometric detection of peptide-loaded monocyte-derived DCs

Monocyte-derived DCs were prepared from PBMCs from DR3/DQ2-positive blood donors as described[21]. DCs were matured using 150 ng/ml LPS for 48 h, supplemented with 40 µM deamidated DQ2.5-glia-α1a after 24 h. Flow cytometric staining and analysis was performed as specified in Supplementary Table 4.

Isolation of single-cell suspensions from duodenal biopsies and small intestinal resections and flow cytometry

Single-cell suspensions from duodenal biopsies or from small intestinal resection were prepared as described[22] and analyzed by flow cytometry as detailed in Supplementary Table 4.

Sorting of PCs, microscopy and ELISPOT

Single-cell suspensions were stained and sorted as described in Supplementary Table 5. Sorted cells (using RPMI1640 without phenol red for microscopy) were spun down, resuspended and incubated at 37°C/5% CO_2 over night before imaging live cells in culture using a 40x NA 0.5 objective on an inverted Leica DM IL microscope equipped with a Axiocam MRc camera (Zeiss). ELISPOT was performed essentially as described[13], except that cells were incubated in the plates for 3 days instead of 1. TG2, gliadin digest or anti-human Ig antibody were coated at 5 µg/ml, 50 µg/ml, and 5 µg/ml, respectively. Chymotrypsin digested gliadin was generated as described[12], with the exception that 20 mM HCl pH 1.7 was used during heating at 95°C for 1h to introduce deamidation. The plate was read

by an ImmunoSpot S5 Analyzer (Cellular Technology Limited). BW 364 T-cells was used as negative control[19].

Antibody modeling and docking to pMHC

Antibody homology models were generated using RosettaAntibody essentially as described[23]. Multiple templates of the V_L–V_H orientation[24] were used, resulting in 10 grafted models. During modeling, the CDR H3 was constrained to the kinked conformation with a harmonic potential[25]. Chothia numbering was used. Models for docking were selected from 2800 Fv models based on low Rosetta energy and good V_L-V_H orientation. Models from at least three different V_L-V_H orientation templates were considered for docking onto HLA-DQ2.5:DQ2.5-glia-α1a (PDB ID 1S9V)[26]). The pMHC structure was "relaxed" in the Rosetta energy function[27]. The top 10 Fv models and the relaxed pMHC structure were prepared for docking by running the ensemble prepack protocol as described[23]. The initial orientation was chosen based on the solved TCR:pMHC interaction (4OZI[28]). Docking using SnugDock[29] consisted of an initial spin around the Ab–Ag center-of-mass axis uniformly sampled from 0 to 360°, and additional random perturbations consisting of small translations and rotations, with values sampled from Gaussian distributions centered at 3 Å and 8°, respectively. During docking, CDR H2 and H3 loops were refined by kinematic loop closure and the V_L-V_H orientation was refined by V_L–V_H docking, generating 1000 models. The final models were picked based on low Rosetta energy, reasonable orientation relative to the pMHC, and agreement with experimentally observed specificities.

Statistics

For comparisons between two groups unpaired two-tailed *t*-test was used. Correlation between pair was determined by linear regression using Pearson correlation to give R^2 and two-tailed p-values. Asterisks were used as follows (also indicated in figure

legends): *$P \leq .05$; **$P \leq .01$; ***$P \leq .001$; ****$P \leq .0001$; ns, not significant. Details on sample size, experimental replicates and statistics are included in the figure legends.

Results

Phage selection of recombinant antibodies highly specific for HLA-DQ2.5 with bound DQ2.5-glia-α1a

To isolate HLA-DQ2.5:DQ2.5-glia-α1a-specific binders, we performed phage selections using a naïve, fully-human scFv-phage library and soluble pMHC molecules[17]. SPR analysis of binding affinity and specificity of purified scFv clones identified 2 lead clones (termed 106 and 107) differing only in one amino acid that bound specifically to HLA-DQ2.5:DQ2.5-glia-α1a, and not to HLA-DQ2.5 with the control peptides DQ2.5-glia-α2 and CLIP2 (Fig. 1A, Supplementary Fig. 1A-C). The scFv clones bound with a monomeric affinity between 70 and 100 nM (Fig. 1A and Supplementary Table 1).

We reformatted and expressed the two scFvs as human IgG1 (hIgG1) mAbs and performed SPR to confirm a gain in functional affinity, resulting in an approximately 160-fold increase in half-life (Supplementary Fig. 1D, E). To confirm DQ2.5-glia-α1a peptide recognition strictly in the context of HLA-DQ2.5, we performed competition ELISA using soluble pMHC and free peptide. Indeed, only soluble HLA-DQ2.5:DQ2.5-glia-α1a, and not peptide alone, competed with the plate-bound complex for binding to the mAbs (Fig. 1B). Of note, DQ2.5-glia-α1a provided as part of a 33mer peptide fragment which binds efficiently to HLA-DQ2.5[30] was not able to inhibit mAb binding to pMHC (Fig. 1C).

Next, we extended the specificity analysis by including 7 HLA-DQ2.5-gluten-peptide complexes in ELISA. This panel included common epitopes from γ- and ω-gliadin to which CD patients mount T-cell responses. Neither of the mAbs bound any of the complexes besides HLA-DQ2.5:DQ2.5-glia-α1a (Fig. 1D), not even the pMHC complex of the highly homologous DQ2.5-glia-ω1. Collectively, these results

show that the mAbs exclusively recognize DQ2.5-glia-α1a bound to HLA-DQ2.5 and are not cross-reactive with HLA-DQ2.5 in complex with the other gluten peptides tested.

Mapping fine-specificity of the candidate mAbs

To validate mAb binding in a cellular context, we utilized murine A20 B cells transduced with HLA-DQ2.5 with covalently linked DQ2.5-glia-α1a or CLIP2 peptides. Both mAbs bound specifically to cells displaying the DQ2.5-glia-α1a epitope, while neither bound CLIP2 (Fig. 2A and Supplementary Fig. 2A).

To further map fine-specificity, we screened for binding against a panel of HLA-DQ2.5:peptide or HLA-DQ2.2:peptide expressing A20 B cells (Supplementary Fig. 2B). Covalent tethering of the peptides to MHC largely eliminates effects of differences in peptide off-rates, enabling comparative assessment of binding. None of the mAbs bound the HLA-DQ2.5:DQ2.5-glia-ω1 or the HLA-DQ2.2:DQ2.5-glia-α1a complexes (Fig. 2B, Supplementary Fig. 2C-E). As DQ2.5-glia-α1a and DQ2.5-glia-ω1 differ at the p7 and p9 positions (Fig. 2C), we constructed pL7Q and pY9F variants of DQ2.5-glia-α1a to resemble DQ2.5-glia-ω1 in these positions. While both mAbs bound the pL7Q variant, albeit not as strongly as DQ2.5-glia-α1a, neither bound the pY9F variant (Fig. 2B). Of the polymorphic residues that differ between HLA-DQ2.5 and HLA-DQ2.2, the α72 residue (S in HLA-DQ2.5 and I in HLA-DQ2.2) is the only residue located so that it could potentially make direct interactions with the mAbs (Fig. 2D). As expected, neither of the mAbs bound the Sα72I variant (Fig. 2B). As seen with soluble HLA molecules, we did not observe binding to DQ2.5-glia-α2 (Fig. 2B). Additionally, the native, non-deamidated DQ2.5-glia-α1a (DQ2.5-glia-α1a-Q) was not recognized.

In an effort to visualize how the mAbs bind pMHC, we built Fv homology models using the V region sequence of mAb 107 and docked the models to the crystal structure of HLA-DQ2.5:DQ2.5-glia-α1a[26]. The three selected docking models were highly similar and positioned the Fv in a TCR-like diagonal manner across the pMHC (Fig. 2D). In all three models, the CDR-H3 was positioned close to p7, and although no direct interactions were identified, the pL7Q substitution could indirectly be

sensed, possibly causing the small reduction in MFI observed (Fig. 2B,E). Similarly, both CDR-L1 and CDR-L3 are in close proximity to p9 (Fig. 2E). In the model, three residues are close enough to interact with the p9Y, and one of these residues potentially forms a H-bond with Sα72 of the MHC, thus, giving a molecular explanation to the lost binding (Fig. 2E). In summary, fine-specificity analysis using single mutant pMHC variants revealed that the mAbs discriminate between highly similar pMHC complexes.

Detection of cell-surface HLA-DQ2.5:DQ2.5-glia-α1a complexes

As all efforts to characterize specificity and affinity of the antibodies were conducted using recombinant HLA-DQ2.5 with peptide covalently tethered with a linker to the N-terminus of DQβ, either soluble or cell-bound, we next examined if the mAbs could bind HLA-DQ2.5^{+} cells loaded with soluble peptide. For this purpose, we isolated monocytes using PBMCs from a healthy HLA-DQ2.5^{+} donor and *in vitro* differentiated to monocyte-derived DCs and loaded the cells with peptide. Using mAb 106, we specifically detected cells presenting DQ2.5-glia-α1a (Supplementary Fig. 3A).

B cells and CD19^{+} PCs are the most abundant DQ2.5-glia-α1a presenting cell subsets in the intestinal mucosa of CD patients

Encouraged by the ability of mAb 106 to specifically stain cells exogenously loaded with DQ2.5-glia-α1a peptide, we generated single-cell suspensions of intestinal biopsies from HLA-DQ2.5^{+} untreated CD patients, and co-stained the freshly isolated cells with mouse IgG2b (mIgG2b) versions of mAb 106 together with antibodies specific for other APC surface markers (Fig. 3A and Supplementary Fig. 3B-D). Unexpectedly, we observed binding of mAb 106 almost exclusively to PCs (large, viable, CD19$^{+/-}$CD27^{+}CD38^{+}) and B cells (smaller, viable, CD19^{+}CD38^{-}), whereas very few CD11c^{+}CD14^{-} DCs and CD11c^{+}CD14^{+} or CD11c^{-}CD14^{+} Mfs stained positive (Fig. 3A). Analysis of three patients in parallel showed an average of 27.4% and 35.4% mAb 106 positive PCs and B cells, respectively. Importantly, pre-blocking of FcγRs did not affect staining (Supplementary Fig. 3D). We also assessed the

abundance of these cells in the LP of CD patients. Cells of the B cell compartment dominated in numbers, while the DCs and the Mf subpopulations were found in low numbers (Fig. 3B). Notably, PCs greatly outnumber the B cells[31].

We then compared the level of peptide presentation by B cells and PCs as detected by mAb 106 or 107 staining of both untreated CD and treated CD patients (i.e. on gluten-free diet) and matched with non-CD healthy controls. Notably, these mAbs stained cells similarly (data not shown). Small intestinal PCs can be separated into 3 major subsets with distinct longevity based on CD19 and CD45 expression; $CD19^+CD45^+$ PCs which are dynamically exchanged, and $CD19^-CD45^+$ PCs and $CD19^-CD45^-$ PCs which are long-lived subsets and exhibit little and no replacement, respectively (we refer to these subsets as $CD19^+$, $CD45^+$, and $CD45^-$ PCs, respectively; Fig. 4A and Supplementary Fig. 4A)[22]. Of these PC subsets, we found the $CD19^+$ PCs to display the highest level of HLA-DQ2.5:DQ2.5-glia-α1a complexes, followed by the $CD45^+$ and the $CD45^-$ PCs, with an average of 19%, 11% and 7% positive cells among HLA-$DQ2.5^+$ untreated CD patients, respectively (Fig. 4B). An average of 16% of the B cells were positive (Fig. 4B). Further analysis of patients revealed that all PC subsets and the B cells of treated CD patients stained negative, comparable to both HLA-$DQ2.5^+$ and HLA-$DQ2.5^-$ healthy controls (Fig. 4C,D and Supplementary Fig. 4B). Additionally, both HLA-$DQ8^+$ and HLA-$DQ2.2^+$ CD patients with active disease were negative. Possibly, there was a higher number of positive PCs from patients with high Marsh scores (Fig. 4E). In summary, we found PCs and B cells to be the main cell types presenting DQ2.5-glia-α1a on HLA-DQ2.5, with the highest level of staining in the $CD19^+$ PC subset.

DQ2.5-glia-α1a presenting PCs express IgA BCR specific for TG2 and gliadin

Ab-secreting cells producing IgA antibodies towards TG2 and gliadin are a hallmark of CD[12,13]. We first determined the BCR isotype of the PCs and found the vast majority to express IgA BCR and the rest to be mainly of IgM isotype (Fig. 5A and Supplementary Fig. 5A), in line with previous descriptions of the intestinal PC compartment[31]. There was no difference between the $pMHC^+$ and $pMHC^-$ PC

populations. We next assessed whether TG2-specific PCs were among the cells detected by the pMHC-specific mAb. From three untreated CD patients, we sorted four populations of PCs; bulk PCs, bulk $TG2^+$ PCs, $pMHC^+TG2^+$ PCs and $pMHC^+TG2^-$ PCs by use of mAb 107 and TG2-antigen multimers. The cells of all four populations were microscopically PCs, being large lymphocytes with eccentric nuclei (Fig. 5B). Further, TG2-specific ELISPOT using the sorted PCs verified that the cells secrete IgA anti-TG2 antibodies (Supplementary Fig. 5B). To perform a further assessment of antigen reactivity of the presenting PCs, we then sorted $pMHC^+$ and $pMHC^-$ PC populations and performed TG2 and gliadin ELISPOT (Fig. 5C and Supplementary Fig. 5C), which showed that both groups contained PCs secreting TG2-specific antibodies, whereas PCs secreting gliadin-specific antibodies could only be detected in the $pMHC^+$ group. Among bulk PCs, spots were visible only at high cell numbers (Supplementary Fig. 5C). This is in line with the observation that approximately 10% of the PCs in the inflamed mucosa of CD patients are TG2-specific[13]. We also evaluated if the pMHC-specific staining level among the $CD19^+$ PCs identified in Fig. 4 would reflect the serum IgA anti-TG2 titer of the patients. We did not find any correlation (Fig. 5D), in line with a previously reported lack of correlation between the frequencies of TG2-specific PCs and serum Ab titers in the intestinal mucosa[32].

Gut PCs express MHCII and co-stimulatory molecules

The specific detection of gluten peptide presentation on HLA-DQ2.5 implies MHCII expression on human intestinal PCs. It is unclear to which extent human gut PCs have the capacity to express MHCII due to Blimp1-mediated silencing[22,33,34]. Thus, to verify class II expression, we performed flow cytometric staining using single-cell suspensions from CD patients, showing that the $CD19^+$, $CD45^+$ and $CD45^-$ PCs indeed express MHCII, albeit at a substantially lower level than DCs and macrophages or B cells (Fig. 6A,B and Supplementary Fig. 6A,B). We detected MHCII expression on approximately 20-30% of the gut PCs, and this was not restricted to the TG2-specific PCs (Fig. 6C,D). Along with the observed stronger pMHC-specific staining within the $CD19^+$ PCs (Fig. 4B-D), this subset also showed

the highest frequency of TG2-specific PCs. Additionally, this subset was the only one where we detected double positive MHCII and TG2-specific PCs (Fig. 6D).

To investigate if MHCII expression is a general feature of gut PCs, and not restricted to the inflamed mucosa of CD patients, we evaluated the MHCII expression on PCs from non-inflamed intestinal mucosa. We either used biopsies from a treated and a potential (Marsh 0 of the duodenum, but symptoms of CD) CD patient or small intestinal resections from patients undergoing Whipple procedure (pancreatoduodenectomy) due to pancreatic cancer. Indeed, we detected MHCII expression to a similar extent as in the CD patient samples (Fig. 6E and Supplementary Fig. 6B). Finally, we assessed gut biopsies for the presence of costimulatory molecules important for T cell interaction. In line with previous observations[35], we found that the DCs and Mfs expressed CD40, CD80 and CD86 only in small subpopulations (Supplementary Fig. 7A), and at lower levels than PCs. PCs of both untreated and treated celiacs expressed high levels of CD40 (Figure 6F). Interestingly, there appeared to be a difference in the CD80 and CD86 profile between celiacs and subjects with non-inflamed tissue. Whereas PCs from non-inflamed tissue showed a clear dichotomous CD80 expression pattern, but no CD86 expression, celiacs expressed no apparent CD80, and medium to low levels of CD86 (Fig. 6F and Supplementary Fig. 7B,C). Taken together, these results show that PCs of the gut express MHCII and co-stimulatory molecules, which suggest that PCs may serve as important APCs in the intestinal mucosa.

Discussion

In this study, we report the generation of mAbs highly specific for HLA-DQ2.5 in complex with one of the immunodominant T-cell epitopes in CD, DQ2.5-glia-α1a. By utilizing these mAbs, we identified B cells and PCs as the most abundant cells presenting gluten peptides in the inflamed intestine of CD patients.

This finding was unexpected as the intestinal APC compartment is dominated by macrophages, with smaller populations of DCs, naïve and memory B cells[8,9,36]. Previous experiments with *in vitro*

gluten peptide-loaded cells isolated from biopsies pointed to a $CD11c^+$ population as particularly efficient APCs[8]. However, no activation was detected without *in vitro* peptide loading, which is in line with our data where we did not detect specific pMHC staining of this cell population, despite high MHCII expression. Furthermore, although the PCs were clearly positive for MHCII, the expression levels are much lower on PCs than on DCs, which may explain why they have been missed in previous studies. Although the affinities of mAbs 106 and 107 are in line with those reported for other TCR-like mAbs isolated from naïve libraries[37,38], it might be too low to detect rare cells. Thus, our lack of detection of macrophages and DC as specific APCs, might in part be explained by low cell density in the intestine[8,9], and possibly by their migration to the mesenteric lymph node after antigen uptake[39]. *In vivo* loaded DCs might well be migratory[9] and thus not present high levels of peptide in the duodenal material assessed.

B cells and PCs expressing Ig specific for gliadin and TG2 are a characteristic of CD[12,13]. The dominant B-cell lineage in the LP is PCs, which are found in high numbers, constituting 25-35% of the total mononuclear cell population, whereas there is only a minor population of memory B cells and very few naïve B cells[36]. In CD, approximately 1% and 10% of the PCs are specific for gliadin or TG2, respectively[12,13]. The role of these cells and the antibodies they produce in disease development have so far not been appreciated, as the PCs have not been considered APCs and a pathogenic role for their secreted antibodies has yet to be shown. Our findings strongly point to PC involvement as APCs for gluten-reactive $CD4^+$ T cells. Comparing the 3 major subsets of small intestinal PCs, we found the $CD19^+$ subset to present DQ2.5-glia-α1a most efficiently. This subset is highly dynamic and undergoes constant renewal, whereas the $CD45^+$ and $CD45^-$ PCs are long-lived, in particular the $CD45^-$ PCs, where we detected little peptide presentation[22]. The finding that the TG2-specific PCs are predominantly $CD19^+$, and thus short-lived, parallels the observation that serum anti-TG2 IgA titers drops upon gluten-free diet[40].

Despite the fact that intestinal IgA^+ PCs appear to have a functional BCR, and thus Ag capture ability, they are thought to lack APC properties due to Blimp1-mediated transcriptional silencing of

the MHCII loci[33,41]. However, we show that intestinal PCs express MHCII, as well as the costimulatory CD40, CD80 and CD86 molecules, which together may give them ability to activate T cells. The presence of IgA^+ DQ2.5-glia-α1a presenting cells among TG2-specific PCs strengthens the so-called hapten-carrier hypothesis as a mechanism to explain how TG2 specific B cells get help from gluten reactive T cells[42,43]. The phenotype of the $CD19^+CD38^-$ B cells we identified has been thoroughly investigated[22,36]. This population was found to constitute mostly memory B cells ($CD27^+IgD^-IgA^+$) with a minor population of naïve-mature B cells ($CD27^-IgD^+IgM^+$) most likely representing a variable contribution from isolated lymphoid follicles and blood.

The ability of PCs to act as APCs is controversial. Whereas murine PCs have been shown to process antigen and activate T cells[44], this has proven much more difficult to verify for human PCs. However, human bone marrow and splenic PCs have been shown to express MHCII[45]. To firmly establish that human gut PCs activate gluten-specific T cells, we will pursue functional testing in T-cell assays. We have only assessed the specific pMHC expression on PCs and B cells at severe inflammation, and thus cannot exclude that DCs and the B-cell compartment serve different functions as potential APCs at different physiological sites, as well as at different stages of gut inflammation. Down these lines, it is interesting that the CD80 versus CD86 expression levels differ on PCs at homeostasis and during inflammation (Fig. 6F vs Supplementary Fig. 7B).

In summary, we describe the isolation and characterization of two mAbs with specificity for one of the immunodominant epitopes in CD, namely HLA-DQ2.5 in complex with DQ2.5-glia-α1a. This particular epitope is usually described as part of the convergent 33mer gluten derived peptide to which the majority of all HLA-$DQ2.5^+$ CD patients respond, and ongoing work aim to elucidate the exact form our Abs bind *in situ*[3,30,46]. Using the mAbs to detect the presence of the target pMHC complex on cells isolated from intestinal lesions of CD patients, they bound to PCs and B cells, and not to macrophages and DCs. Although life-long gluten-free diet is a safe treatment for many CD patients, there is also an unmet medical need for novel treatments. Our data identify PCs of the gut

as the most prevalent gluten peptide presenting cell in the CD gut mucosa, which indicates that gut PCs may well function as an APC, and thus constituting a potential therapeutic target in CD.

A potential role of PCs as APCs and the establishment of the importance of B cells in presentation of gluten peptide may also offer instructive clues for our understanding other T-cell driven autoimmune diseases. Lastly, we found the ability of the PCs to express MHCII was not restricted to the inflamed mucosa of CD patients, which has important implications for our understanding of mucosal adaptive immunity.

Figure legends

Figure 1. Binding properties of the lead HLA-DQ2.5:DQ2.5-glia-αIa-specific binders. (*A*) Representative SPR single-cycle kinetics sensorgrams of the lead scFv clones 106 and 107 for binding to HLA-DQ2.5:DQ2.5-glia-αIa (n=2-3). K_D values were derived by fitting the data to a 1:1 Langmuir model. Steady state affinity evaluations are shown as inset figures. (*B-D*) The scFv clones and isotype control scFv (anti-NIP) were reformatted to hIgG1 mAbs, expressed and purified before assessment of specificity. (*B,C*) Competition ELISAs where the hIgG1 mAbs were pre-incubated with titrated amounts of (*B*) soluble pMHCs, HLA-DQ2.5:DQ2.5-glia-α1a and HLA-DQ2.5:DQ2.5-glia-α2, or the corresponding free peptides, and (*C*) 33mer α-gliadin before assessment of ability to compete with binding to plate-bound HLA-DQ2.5:DQ2.5-glia-α1a (n=3). (*D*) Eight different HLA-DQ2.5:gluten peptide complexes and HLA-DQ2.5:CLIP2 were used in ELISA for specificity analysis (n=2). mAb 2.12.E11 specific for the β-chain of HLA-DQ2 was included to control pMHC capture levels. Error bars illustrate mean ± SD of duplicates.

Figure 2. Mapping the fine-specificity and the structural basis for specificity. (*A,B*) Flow cytometric analysis of A20 B cells expressing HLA-DQ2 with covalently bound peptides. (*A*) Binding to cells expressing HLA-DQ2.5 with DQ2.5-glia-α1a or CLIP2 peptides (n=2). (*B*) Binding to a panel of cells expressing HLA-DQ2.5:peptide or HLA-DQ2.2:peptide. Data are shown as ratio median fluorescent intensity (MFI) compared to isotype control mAb (n=2). Q indicate native (glutamine) DQ2.5-glia-α1a epitope. Unless specified, all peptides were tested in their deamidated form. (C) Alignment and structural conformation of MHC-bound DQ2.5-glia-α1a (green) and DQ2.5-glia-ω1 (cyan). Residues differing are underlined in the peptide sequences. Structure of DQ2.5-glia-α1a is based on PDB ID 1S9V while the structure of DQ2.5-glia-ω1 is modeled. (*D*) Overlay of the top three docking models of the Fvs onto HLA-DQ2.5:DQ2.5-glia-α1a[26]. Peptide residues mutated for fine-specificity analysis and the HLA-DQ2.5/DQ2.2 polymorphism at Sα72 is illustrated. (*E*) Fv residues from the three models that are within 5 Å of p7, p9 and Sα72 are shown. (*D-E*) Coloring as follows: V_H and V_L, black; MHCα,

grey; MHCβ, light orange; DQ2.5-glia-α1a, green; CDR-H1 and CDR-H2, deep purple; CDR-H3, red; CDR-L1 and CDR-L2, deep teal; CDR-L3, blue; Sα72, pink; p7 and p9, pale green; H-bonds, yellow dashes.

Figure 3. Specific detection of gluten peptide presentation in context of HLA-DQ2.5 and the abundance of the cell populations in the LP. (*A*) Single-cell suspensions of intestinal biopsies obtained from patients undergoing gastroduodenoscopy were stained with a panel of antibodies to phenotypically characterize DQ2.5-glia-α1a presenting cells along with mIgG2b 106. Bound mAb 106 was detected using a FITC-conjugated secondary anti-mouse IgG2b Ab. Samples from three HLA-DQ2.5^{+} untreated CD (UCD) patients with Marsh 3B/C were run in parallel and a representative example is shown. The mean percent of mAb 106 positive cells from the three patients compared to no primary antibody is shown ± SD. (*B*) The abundance of the cell populations identified in panel A was determined relative to percentage of live cells in samples from HLA-DQ2.5^{+} UCD patients (Marsh 3A/B/C, n=6). Each data point represents an individual subject. Error bars illustrate mean ± SD.

Figure 4. PCs and B cells of gut biopsies present the DQ2.5-glia-α1a peptide. Detection of DQ2.5-glia-α1a presentation among PCs and B cells in single-cells suspension prepared from intestinal biopsies from either untreated CD (UCD) or treated CD (TCD) patients or healthy controls. mIgG2b mAb 106 or 107 were used for detection and percent positive cells was determined relative to use of secondary antibody alone. (*A*) Representative flow cytometric gating strategy to identify PCs and B cells from single-cell suspensions. (*B*) Percentage of specific HLA-DQ2.5:DQ2.5-glia-α1a detection among PC subsets and B cells in HLA-DQ2.5^{+} UCD CD patients (n=18) compared to controls (grouped healthy and non-HLA-DQ2.5^{+} CD patients, n=15). Two-tailed *P*-values are shown (unpaired t-test). (*C*) Stratification of the control patients among the CD19^{+} PCs from panel B. Ctrl HLA-DQ2.5^{+} (n=5), Ctrl HLA-DQ2.5^{-} (n=5), UCD HLA-DQ2.5^{+} (n=18), TCD HLA-DQ2.5^{+} (n=3), UCD HLA-DQ8^{+} (n=1), and UCD HLA-DQ2.2^{+} (n=1). (*D*) Representative histograms showing pMHC-specific staining within patient

groups as indicated. (*E*) The HLA-DQ2.5$^+$ UCD patients (n=18) were stratified according to Marsh score as indicated. (*B-E*) Non-CD ctrl patients did not have mucosal alterations. Each data point represents an individual subject. Red bars indicate mean percentage.

Figure 5. DQ2.5-glia-α1a presenting PCs express TG2- and gliadin-specific IgA. (*A*) Expression profile of surface IgA and IgM BCR on CD38$^+$ PCs staining as pMHC$^+$ or pMHC$^-$ (HLA-DQ2.5$^+$ UCD patients with Marsh 3B/C, n=3). Error bars illustrate mean ± SD. (*B*) Representative micrographs of FACS-sorted PCs subsets as indicated (HLA-DQ2.5$^+$ UCD patients with positive serum anti-TG2 IgA titers and with Marsh 3B/C, n=3). Two individual cells within each group are shown. (*C*) TG2 and gliadin ELISPOT on FACS sorted pMHC$^+$ or pMHC$^-$ CD38$^+$ PCs subsets as indicated (HLA-DQ2.5$^+$ UCD patients with Marsh 3B/C, n=2). TG2- and gliadin-specific IgA antibodies were detected using AP-conjugated anti-IgA Ab. (*D*) Percentage of HLA-DQ2.5:DQ2.5-glia-α1a detection within CD19$^+$ PCs does not correlate with serum anti-TG2 IgA titer (n=18). Each data point represents an individual subject and the Marsh score is indicated. The dotted line indicates upper and lower thresholds for anti-TG2 IgA detection (7 and 120, respectively). The line is derived from linear fitting; R^2 and two-tailed *P*-values of IgA anti-TG2 antibody value (Pearson correlation); ns=not significant.

Figure 6. Gut PCs express MHCII and costimulatory molecules. (*A-D*) Single-cell suspensions from five HLA-DQ2.5$^+$ UCD patients all with positive serum anti-TG2 IgA antibody levels and with Marsh score 3A/B/C were assessed for MHCII expression and TG2 specificity (n=5). (*A*) Percentage MHCII expression among various cell subsets as indicated compared to isotype control mAb. (*B*) Representative histograms showing MHCII-specific staining within cell subsets as indicated. The bulk CD38$^+$ PC population was used to represent the isotype staining for all three PC subsets. (*C*) Representative overview of MHC and anti-TG2 BCR staining among the PC subsets. Percent positive cells within quadrant are indicated. (*D*) Distributions of cells stained as single MHCII$^+$, single TG2$^+$ or double MHCII$^+$TG2$^+$ within the PCs subsets as seen in (C). Background staining (Bg) was determined

based on isotype control mAb for the MHCII staining and without TG2 multimer for the anti-TG2 BCR staining. (*E*) Percentage MHCII expression on PC subsets from non-inflamed intestinal samples (n=6). Cells were obtained either from patients undergoing Whipple procedure (Whipple, n=4) or a treated CD patient (TCD, n=1) or a potential CD patient (potential CD, n=1, non-inflamed duodenum, but symptoms of CD). All subjects were evaluated to have normal histology of the duodenum. (*F*) Representative staining for costimulatory markers CD40, CD80 and CD86 on PCs from UCD or TCD patients (n=4, 3 HLA-DQ2.5^{+} UCD patients with Marsh 3A/B and 1 TCD with Marsh 0). Red bars indicate mean percentage. Error bars indicate mean ± SD. Each data point represents an individual subject; two-tailed *P*-values from unpaired t-test.

References

1 Sollid LM , Jabri B. Triggers and drivers of autoimmunity: lessons from coeliac disease. Nat Rev Immunol **13**, 294-302, doi:10.1038/nri3407 (2013).

2 Abadie V, Sollid LM, Barreiro LB, et al. Integration of genetic and immunological insights into a model of celiac disease pathogenesis. Annu Rev Immunol **29**, 493-525, doi:10.1146/annurev-immunol-040210-092915 (2011).

3 **Tye-Din JA, Stewart JA, Dromey JA, Beissbarth T**, et al. Comprehensive, quantitative mapping of T cell epitopes in gluten in celiac disease. Sci Transl Med **2**, 41ra51, doi:10.1126/scitranslmed.3001012 (2010).

4 Arentz-Hansen H, Korner R, Molberg O, et al. The intestinal T cell response to alpha-gliadin in adult celiac disease is focused on a single deamidated glutamine targeted by tissue transglutaminase. J Exp Med **191**, 603-612 (2000).

5 Xia J, Sollid LM & Khosla C. Equilibrium and kinetic analysis of the unusual binding behavior of a highly immunogenic gluten peptide to HLA-DQ2. Biochemistry **44**, 4442-4449, doi:10.1021/bi047747c (2005).

6 Fallang LE, Bergseng E, Hotta K, et al. Differences in the risk of celiac disease associated with HLA-DQ2.5 or HLA-DQ2.2 are related to sustained gluten antigen presentation. Nat Immunol **10**, 1096-1101, doi:10.1038/ni.1780 (2009).

7 Mowat AM , Agace WW. Regional specialization within the intestinal immune system. Nat Rev Immunol **14**, 667-685, doi:10.1038/nri3738 (2014).

8 Raki M, Tollefsen S, Molberg Ø, et al. A unique dendritic cell subset accumulates in the celiac lesion and efficiently activates gluten-reactive T cells. Gastroenterology **131**, 428-438, doi:10.1053/j.gastro.2006.06.002 (2006).

9 Beitnes AC, Raki M, Lundin KE, et al. Density of CD163+ CD11c+ dendritic cells increases and CD103+ dendritic cells decreases in the coeliac lesion. Scand J Immunol **74**, 186-194, doi:10.1111/j.1365-3083.2011.02549.x (2011).

10 **Bujko A, Atlasy N**, Landsverk OJB, et al. Transcriptional and functional profiling defines human small intestinal macrophage subsets. J Exp Med **215**, 441-458, doi:10.1084/jem.20170057 (2018).

11 Beitnes AC, Raki M, Brottveit M, et al. Rapid accumulation of CD14+CD11c+ dendritic cells in gut mucosa of celiac disease after in vivo gluten challenge. PLoS One **7**, e33556, doi:10.1371/journal.pone.0033556 (2012).

12 Steinsbø Ø, Henry Dunand CJ, Huang M, et al. Restricted VH/VL usage and limited mutations in gluten-specific IgA of coeliac disease lesion plasma cells. Nat Commun **5**, 4041, doi:10.1038/ncomms5041 (2014).

13 Di Niro R, Mesin L, Zheng NY, et al. High abundance of plasma cells secreting transglutaminase 2-specific IgA autoantibodies with limited somatic hypermutation in celiac disease intestinal lesions. Nat Med **18**, 441-445, doi:10.1038/nm.2656 (2012).

14 Chen D, Ireland SJ, Davis LS, et al. Autoreactive CD19+CD20- Plasma Cells Contribute to Disease Severity of Experimental Autoimmune Encephalomyelitis. J Immunol **196**, 1541-1549, doi:10.4049/jimmunol.1501376 (2016).

15 Li R, Patterson KR & Bar-Or A. Reassessing B cell contributions in multiple sclerosis. Nat Immunol, doi:10.1038/s41590-018-0135-x (2018).

16 Ludvigsson JF, Bai JC, Biagi F, et al. Diagnosis and management of adult coeliac disease: guidelines from the British Society of Gastroenterology. Gut **63**, 1210-1228, doi:10.1136/gutjnl-2013-306578 (2014).

17 Løset GA, Lobersli I, Kavlie A, et al. Construction, evaluation and refinement of a large human antibody phage library based on the IgD and IgM variable gene repertoire. J Immunol Methods **299**, 47-62, doi:10.1016/j.jim.2005.01.014 (2005).

18 **Høydahl LS, Nilssen NR**, Gunnarsen KS, et al. Multivalent pIX phage display selects for distinct and improved antibody properties. Sci Rep **6**, 39066, doi:10.1038/srep39066 (2016).
19 **Gunnarsen KS, Høydahl LS**, Risnes LF, et al. A TCRalpha framework-centered codon shapes a biased T cell repertoire through direct MHC and CDR3beta interactions. JCI Insight **2**, doi:10.1172/jci.insight.95193 (2017).
20 Berntzen G, Lunde E, Flobakk M, et al. Prolonged and increased expression of soluble Fc receptors, IgG and a TCR-Ig fusion protein by transiently transfected adherent 293E cells. J Immunol Methods **298**, 93-104, doi:10.1016/j.jim.2005.01.002 (2005).
21 Qiao SW, Bergseng E, Molberg Ø, et al. Antigen presentation to celiac lesion-derived T cells of a 33-mer gliadin peptide naturally formed by gastrointestinal digestion. J Immunol **173**, 1757-1762 (2004).
22 Landsverk OJ, Snir O, Casado RB, et al. Antibody-secreting plasma cells persist for decades in human intestine. J Exp Med **214**, 309-317, doi:10.1084/jem.20161590 (2017).
23 **Weitzner BD, Jeliazkov JR, Lyskov S**, et al. Modeling and docking of antibody structures with Rosetta. Nat Protoc **12**, 401-416, doi:10.1038/nprot.2016.180 (2017).
24 Marze NA, Lyskov S & Gray JJ. Improved prediction of antibody VL-VH orientation. Protein Eng Des Sel **29**, 409-418, doi:10.1093/protein/gzw013 (2016).
25 Weitzner BD , Gray JJ. Accurate Structure Prediction of CDR H3 Loops Enabled by a Novel Structure-Based C-Terminal Constraint. J Immunol **198**, 505-515, doi:10.4049/jimmunol.1601137 (2017).
26 **Kim CY, Quarsten H**, Bergseng E, et al. Structural basis for HLA-DQ2-mediated presentation of gluten epitopes in celiac disease. Proc Natl Acad Sci U S A **101**, 4175-4179, doi:10.1073/pnas.0306885101 (2004).
27 **Conway P, Tyka MD**, DiMaio F, et al. Relaxation of backbone bond geometry improves protein energy landscape modeling. Protein Sci **23**, 47-55, doi:10.1002/pro.2389 (2014).
28 **Petersen J, Montserrat V**, Mujico JR, et al. T-cell receptor recognition of HLA-DQ2-gliadin complexes associated with celiac disease. Nat Struct Mol Biol **21**, 480-488, doi:10.1038/nsmb.2817 (2014).
29 Sircar A , Gray JJ. SnugDock: paratope structural optimization during antibody-antigen docking compensates for errors in antibody homology models. PLoS Comput Biol **6**, e1000644, doi:10.1371/journal.pcbi.1000644 (2010).
30 Shan L, Molberg Ø, Parrot I, et al. Structural basis for gluten intolerance in celiac sprue. Science **297**, 2275-2279, doi:10.1126/science.1074129 (2002).
31 Brandtzaeg P , Johansen FE. Mucosal B cells: phenotypic characteristics, transcriptional regulation, and homing properties. Immunol Rev **206**, 32-63, doi:10.1111/j.0105-2896.2005.00283.x (2005).
32 Di Niro R, Snir O, Kaukinen K, et al. Responsive population dynamics and wide seeding into the duodenal lamina propria of transglutaminase-2-specific plasma cells in celiac disease. Mucosal Immunol **9**, 254-264, doi:10.1038/mi.2015.57 (2016).
33 Pinto D, Montani E, Bolli M, et al. A functional BCR in human IgA and IgM plasma cells. Blood **121**, 4110-4114, doi:10.1182/blood-2012-09-459289 (2013).
34 **Piskurich JF, Lin KI**, Lin Y, et al. BLIMP-I mediates extinction of major histocompatibility class II transactivator expression in plasma cells. Nat Immunol **1**, 526-532, doi:10.1038/82788 (2000).
35 Chirdo FG, Millington OR, Beacock-Sharp H, et al. Immunomodulatory dendritic cells in intestinal lamina propria. Eur J Immunol **35**, 1831-1840, doi:10.1002/eji.200425882 (2005).
36 Farstad IN, Carlsen H, Morton HC, et al. Immunoglobulin A cell distribution in the human small intestine: phenotypic and functional characteristics. Immunology **101**, 354-363 (2000).
37 Chames P, Hufton SE, Coulie PG, et al. Direct selection of a human antibody fragment directed against the tumor T-cell epitope HLA-A1-MAGE-A1 from a nonimmunized phage-Fab library. Proc Natl Acad Sci U S A **97**, 7969-7974 (2000).

38 Dahan R, Gebe JA, Preisinger A, et al. Antigen-specific immunomodulation for type 1 diabetes by novel recombinant antibodies directed against diabetes-associates auto-reactive T cell epitope. J Autoimmun **47**, 83-93, doi:10.1016/j.jaut.2013.08.009 (2013).
39 Du Pre MF, Kozijn AE, van Berkel LA, et al. Tolerance to ingested deamidated gliadin in mice is maintained by splenic, type 1 regulatory T cells. Gastroenterology **141**, 610-620, 620 e611-612, doi:10.1053/j.gastro.2011.04.048 (2011).
40 Sulkanen S, Halttunen T, Laurila K, et al. Tissue transglutaminase autoantibody enzyme-linked immunosorbent assay in detecting celiac disease. Gastroenterology **115**, 1322-1328 (1998).
41 Tellier J, Shi W, Minnich M, et al. Blimp-1 controls plasma cell function through the regulation of immunoglobulin secretion and the unfolded protein response. Nat Immunol **17**, 323-330, doi:10.1038/ni.3348 (2016).
42 Sollid LM, Molberg Ø, McAdam S, et al. Autoantibodies in coeliac disease: tissue transglutaminase--guilt by association? Gut **41**, 851-852 (1997).
43 Iversen R, Fleur du Pre M, Di Niro R, et al. Igs as Substrates for Transglutaminase 2: Implications for Autoantibody Production in Celiac Disease. J Immunol **195**, 5159-5168, doi:10.4049/jimmunol.1501363 (2015).
44 Pelletier N, McHeyzer-Williams LJ, Wong KA, et al. Plasma cells negatively regulate the follicular helper T cell program. Nat Immunol **11**, 1110-1118, doi:10.1038/ni.1954 (2010).
45 Ellyard JI, Avery DT, Phan TG, et al. Antigen-selected, immunoglobulin-secreting cells persist in human spleen and bone marrow. Blood **103**, 3805-3812, doi:10.1182/blood-2003-09-3109 (2004).
46 **Bodd M, Ráki M**, Bergseng E, et al. Direct cloning and tetramer staining to measure the frequency of intestinal gluten-reactive T cells in celiac disease. Eur J Immunol **43**, 2605-2612, doi:10.1002/eji.201343382 (2013).

Author names in bold designate shared co-first authorship.

Figure 1

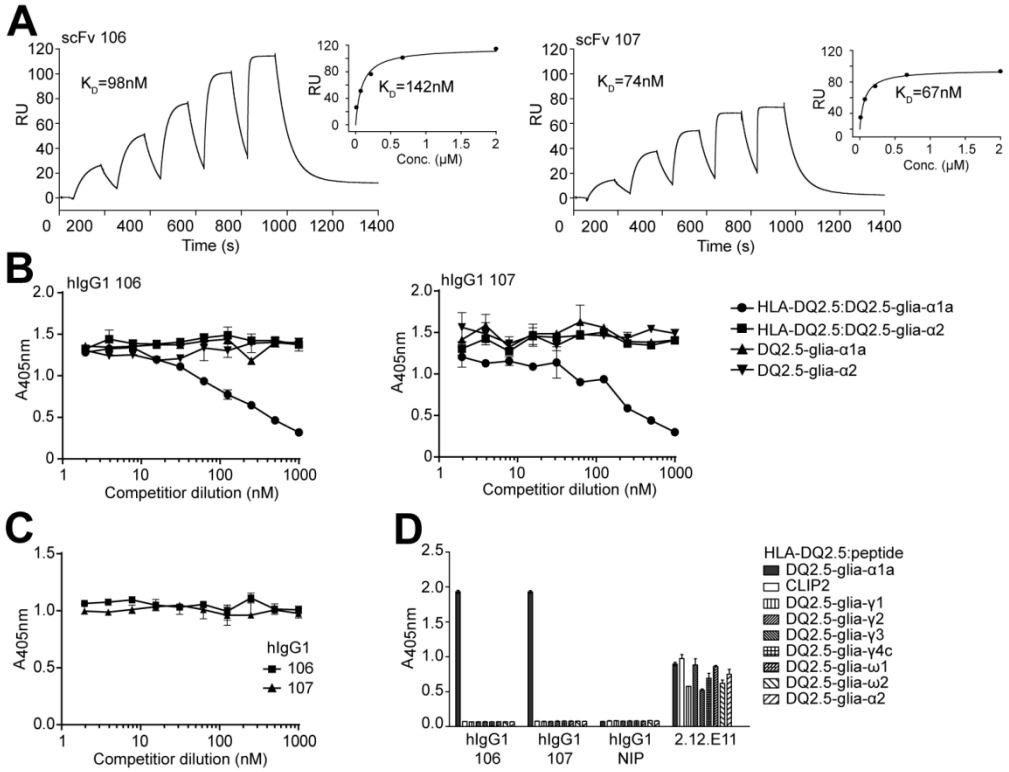
A
scFv 106
K_D=98nM
RU
Time (s)
K_D=142nM
Conc. (μM)
scFv 107
K_D=74nM
K_D=67nM
B
hIgG1 106
hIgG1 107
A405nm
Competitior dilution (nM)
HLA-DQ2.5:DQ2.5-glia-α1a
HLA-DQ2.5:DQ2.5-glia-α2
DQ2.5-glia-α1a
DQ2.5-glia-α2
C
hIgG1
106
107
D
HLA-DQ2.5:peptide
DQ2.5-glia-α1a
CLIP2
DQ2.5-glia-γ1
DQ2.5-glia-γ2
DQ2.5-glia-γ3
DQ2.5-glia-γ4c
DQ2.5-glia-ω1
DQ2.5-glia-ω2
DQ2.5-glia-α2
hIgG1 106
hIgG1 107
hIgG1 NIP
2.12.E11

Figure 2

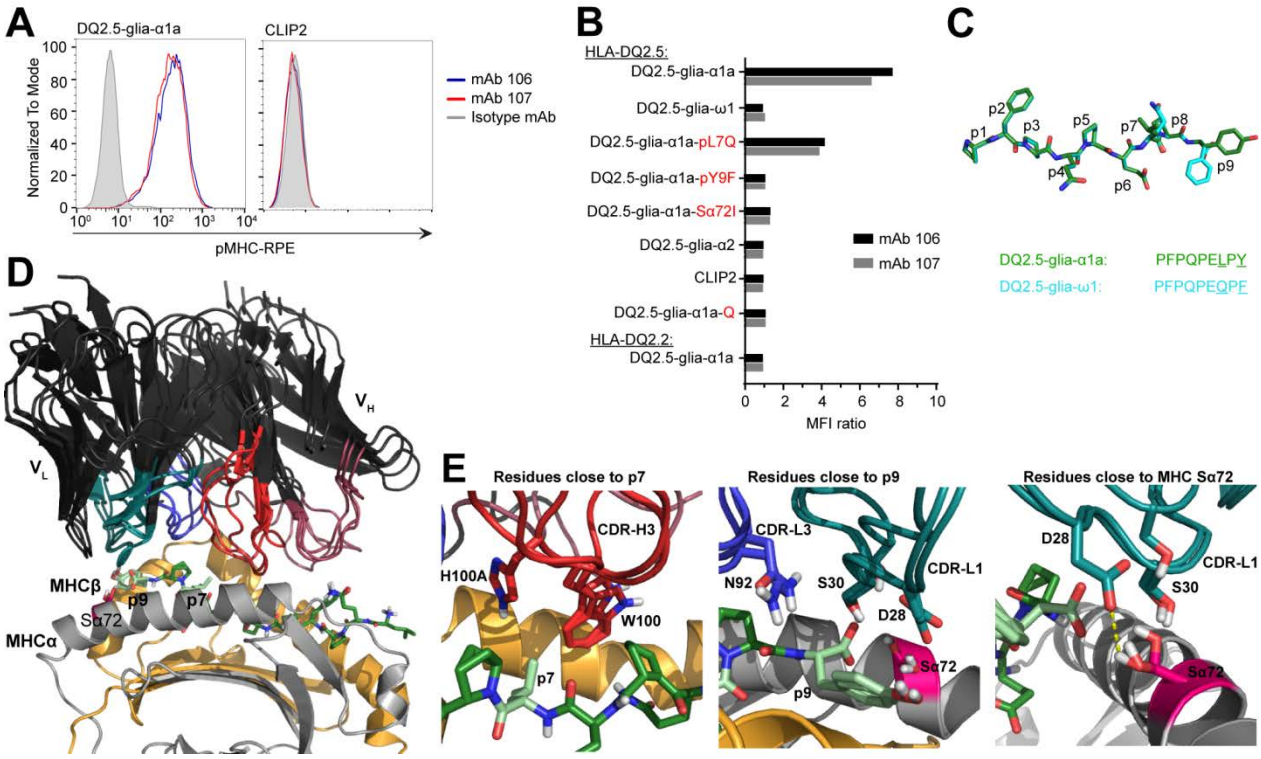
A
DQ2.5-glia-α1a
CLIP2
Normalized To Mode
pMHC-RPE
mAb 106
mAb 107
Isotype mAb
B
HLA-DQ2.5:
DQ2.5-glia-α1a
DQ2.5-glia-ω1
DQ2.5-glia-α1a-pL7Q
DQ2.5-glia-α1a-pY9F
DQ2.5-glia-α1a-Sα72I
DQ2.5-glia-α2
CLIP2
DQ2.5-glia-α1a-Q
HLA-DQ2.2:
DQ2.5-glia-α1a
MFI ratio
C
DQ2.5-glia-α1a: PFPQPELPY
DQ2.5-glia-ω1: PFPQPEQPF
D
V_H
V_L
MHCβ
MHCα
p9
p7
Sα72
E
Residues close to p7
CDR-H3
H100A
W100
Residues close to p9
CDR-L3
CDR-L1
N92
S30
D28
Residues close to MHC Sα72
D28
CDR-L1
S30
Sα72

Figure 3

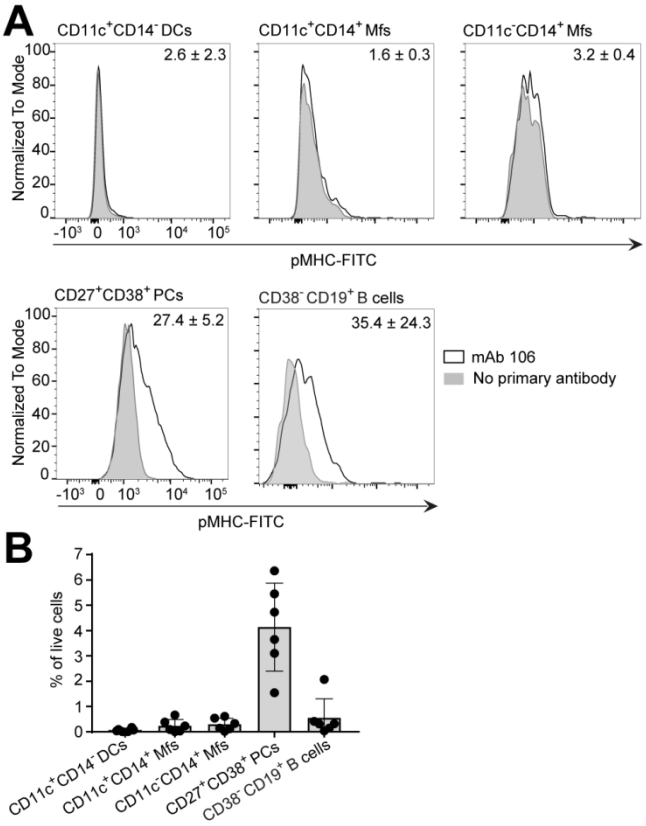
A
CD11c+CD14- DCs
CD11c+CD14+ Mfs
CD11c-CD14+ Mfs
2.6 ± 2.3
1.6 ± 0.3
3.2 ± 0.4
Normalized To Mode
pMHC-FITC
CD27+CD38+ PCs
CD38- CD19+ B cells
27.4 ± 5.2
35.4 ± 24.3
mAb 106
No primary antibody
B
% of live cells
CD11c+CD14- DCs
CD11c+CD14+ Mfs
CD11c-CD14+ Mfs
CD27+CD38+ PCs
CD38- CD19+ B cells

Figure 4

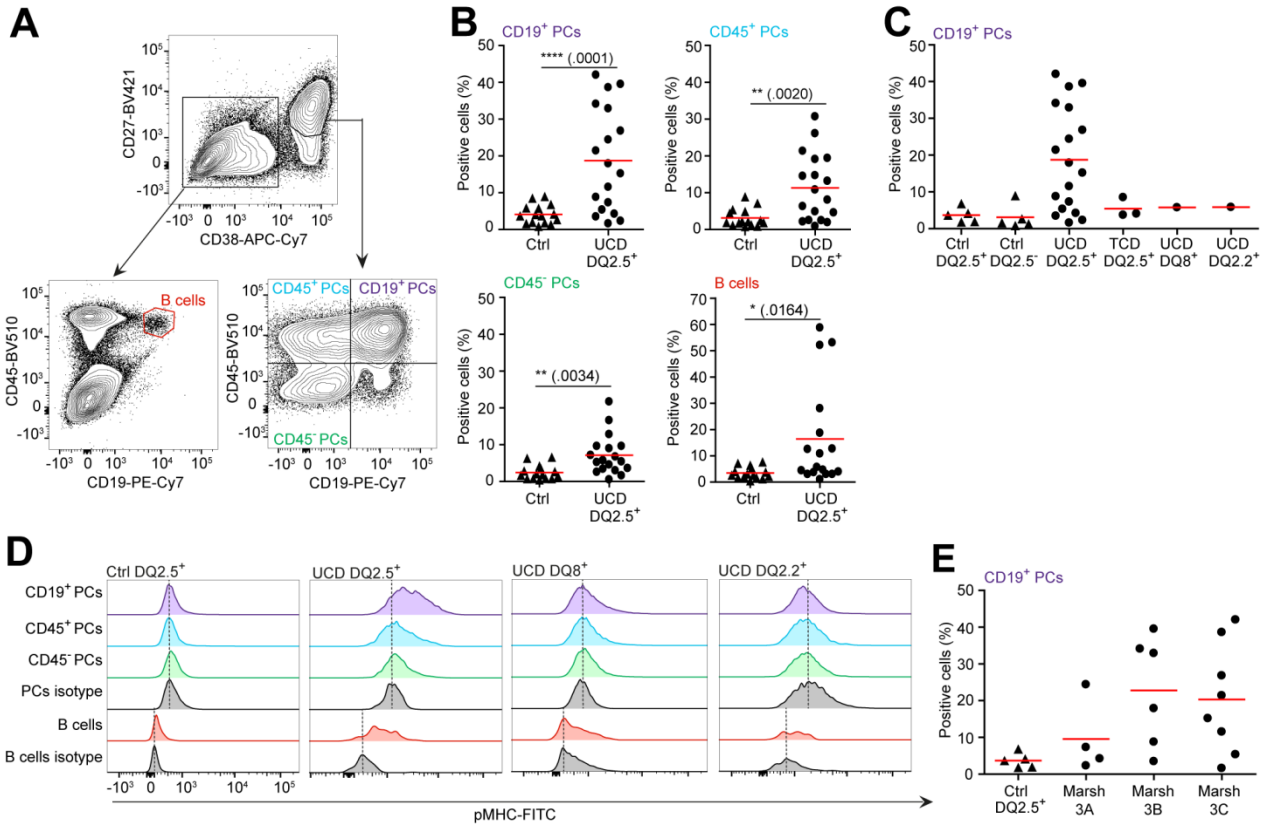
A
CD27-BV421
CD38-APC-Cy7
B cells
CD45-BV510
CD19-PE-Cy7
CD45+ PCs
CD19+ PCs
CD45- PCs
B
CD19+ PCs
CD45+ PCs
CD45- PCs
B cells
Positive cells (%)
**** (.0001)
** (.0020)
** (.0034)
* (.0164)
Ctrl
UCD DQ2.5+
C
CD19+ PCs
Ctrl DQ2.5+
Ctrl DQ2.5-
UCD DQ2.5+
TCD DQ2.5+
UCD DQ8+
UCD DQ2.2+
D
Ctrl DQ2.5+
UCD DQ2.5+
UCD DQ8+
UCD DQ2.2+
CD19+ PCs
CD45+ PCs
CD45- PCs
PCs isotype
B cells
B cells isotype
pMHC-FITC
E
CD19+ PCs
Positive cells (%)
Ctrl DQ2.5+
Marsh 3A
Marsh 3B
Marsh 3C

Figure 5

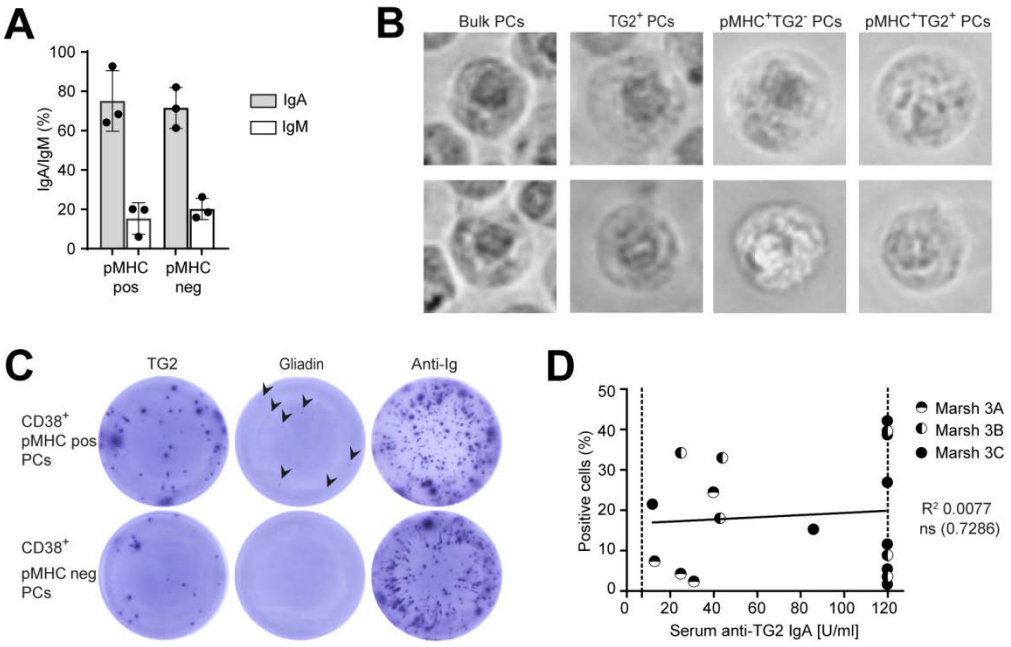
A
IgA/IgM (%)
100
80
60
40
20
0
pMHC pos
pMHC neg
IgA
IgM
B
Bulk PCs
TG2+ PCs
pMHC+TG2- PCs
pMHC+TG2+ PCs
C
TG2
Gliadin
Anti-Ig
CD38+ pMHC pos PCs
CD38+ pMHC neg PCs
D
Positive cells (%)
50
40
30
20
10
0
0
20
40
60
80
100
120
Serum anti-TG2 IgA [U/ml]
Marsh 3A
Marsh 3B
Marsh 3C
R2 0.0077
ns (0.7286)

Figure 6

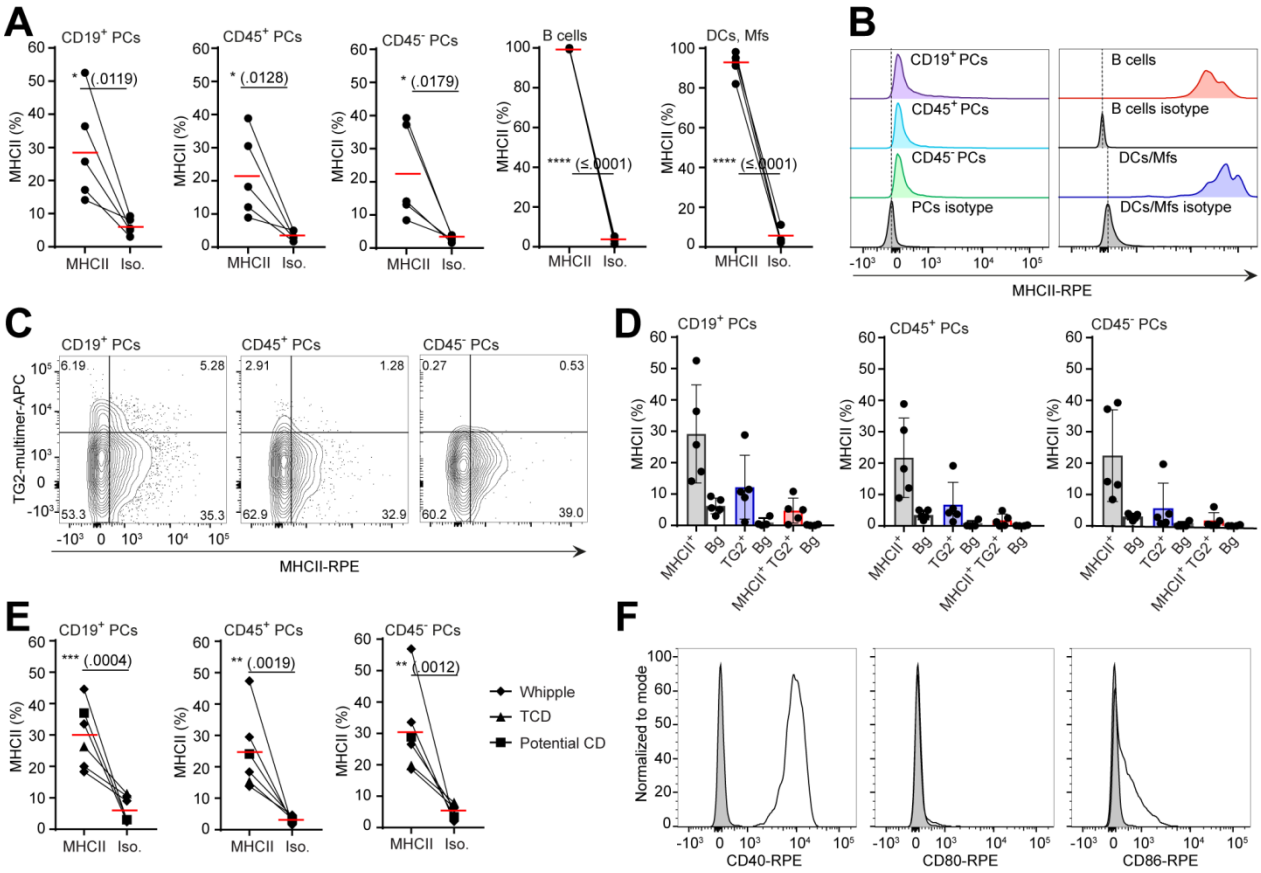
A
CD19+ PCs
CD45+ PCs
CD45- PCs
B cells
DCs, Mfs
MHCII (%)
MHCII Iso.
* (.0119)
* (.0128)
* (.0179)
**** (≤.0001)
B
CD19+ PCs
CD45+ PCs
CD45- PCs
PCs isotype
B cells
B cells isotype
DCs/Mfs
DCs/Mfs isotype
MHCII-RPE
C
CD19+ PCs
CD45+ PCs
CD45- PCs
TG2-multimer-APC
6.19
5.28
53.3
35.3
2.91
1.28
62.9
32.9
0.27
0.53
60.2
39.0
MHCII-RPE
D
CD19+ PCs
CD45+ PCs
CD45- PCs
MHCII+
Bg
TG2+
MHCII+ TG2+
E
CD19+ PCs
CD45+ PCs
CD45- PCs
*** (.0004)
** (.0019)
** (.0012)
Whipple
TCD
Potential CD
F
Normalized to mode
CD40-RPE
CD80-RPE
CD86-RPE

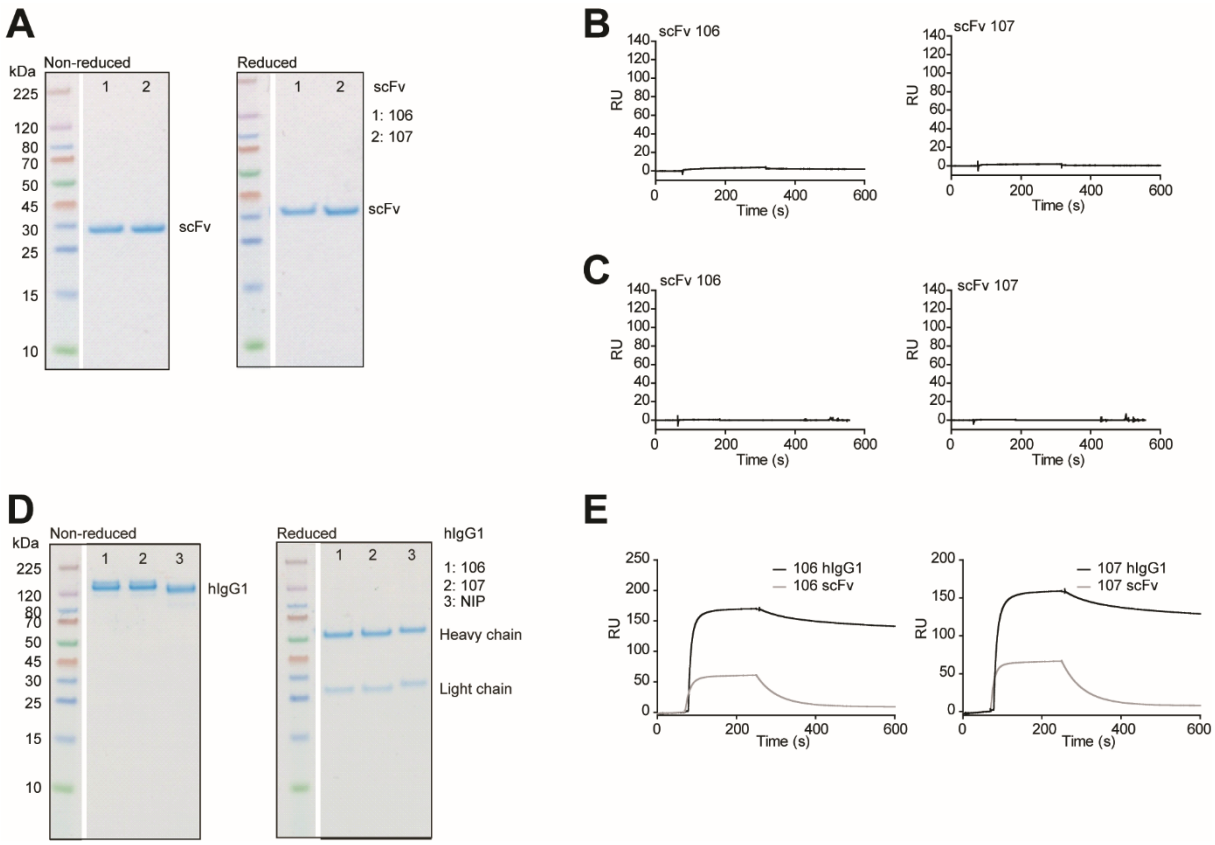

Supplementary Figure 1. Expression and binding of scFv clones and hIgG1 mAbs. (*A*-*C*) The lead scFv clones were expressed and purified from *E. coli* periplasmic fractions. (*A*) SDS-PAGE gel analysis of the scFv clones that specifically bound HLA-DQ2.5:DQ2.5-glia-α1a. Gels were run after purification by IMAC and size exclusion chromatography under non-reducing and reducing conditions. scFv size of approx. 30 kDa is indicated. (*B,C*) Representative SPR sensorgrams of the scFv clones for binding to (*B*) HLA-DQ2.5:CLIP2 (n=2) and (*C*) HLA-DQ2.5:DQ2.5-glia-α2 (n=2). (*D,E*) The lead scFv clones and isotype control scFv (anti-NIP) were reformatted to hIgG1 mAbs, expressed by transient transfection of HEK293E cells and purified from supernatants. (*D*) SDS-PAGE gel of purified hIgG1 mAbs run under non-reducing and reducing conditions. Appropriate-size bands at about 150 kDa for full-length hIgG1 and bands at 50 kDa and 23 kDa (reduced heavy and light chains, respectively) are indicated. (*E*) SPR sensorgrams of hIgG1 mAbs and the corresponding scFv clones binding to HLA-DQ2.5:DQ2.5-glia-α1a to validate gain in functional affinity after reformatting to full-length hIgG1 mAbs.

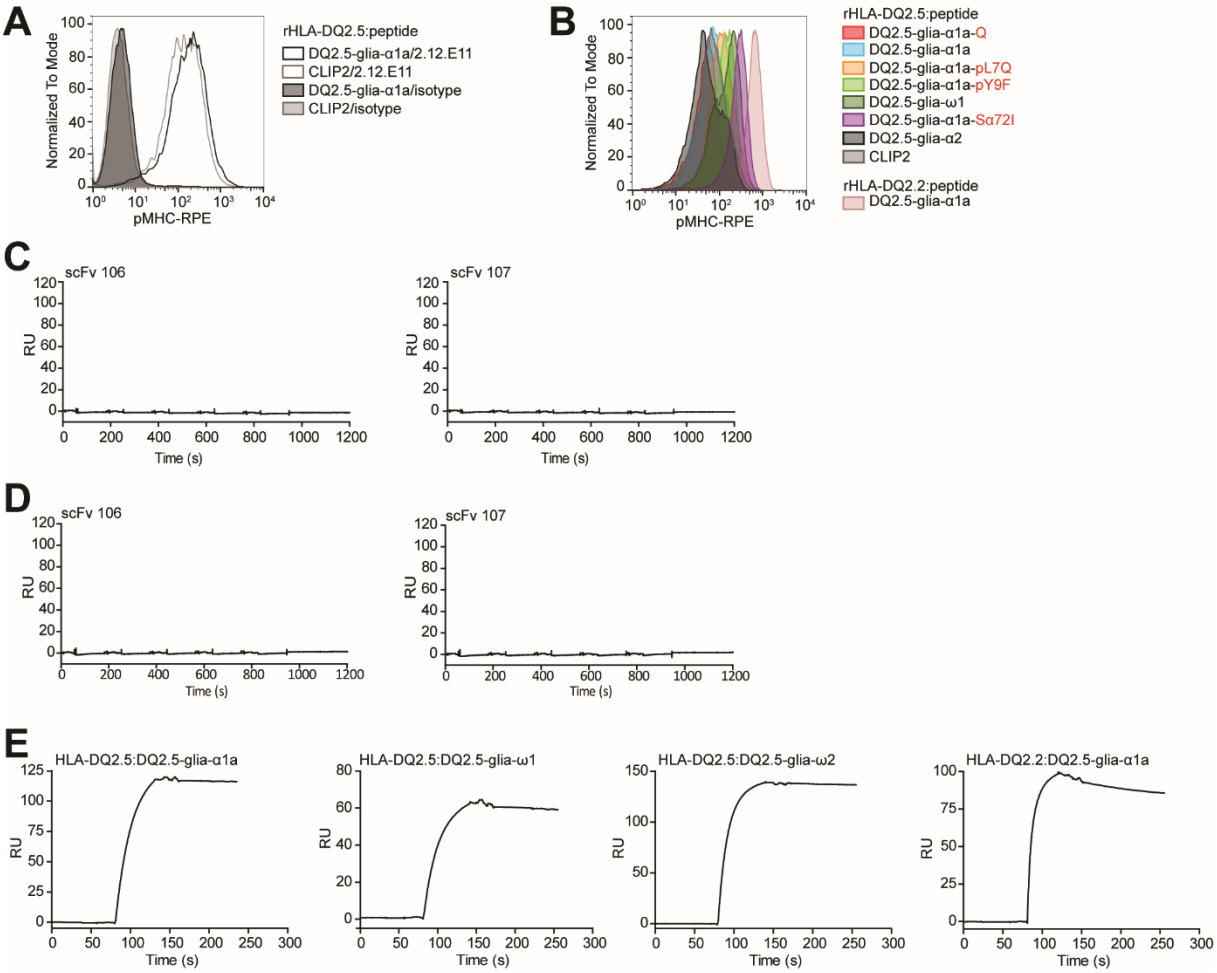

Supplementary Figure 2. Fine-specificity assessment. (*A*) Flow cytometric analysis of A20 B cells transduced to express HLA-DQ2.5 with covalently bound DQ2.5-glia-α1a or CLIP2 peptides stained with biotinylated mAb 2.12.E11 or isotype control mAb, followed by RPE-conjugated streptavidin (n=2). (*B*) Flow cytometric assessment of the pMHC expression level of the panel of A20 B cells transduced with either HLA-DQ2.5 or HLA-DQ2.2 with covalently bound peptide. Q indicates native (glutamine) DQ2.5-glia-α1a epitope. Unless specified, all epitopes are in the deamidated form. All cells were stained with biotinylated mAb 2.12.E11 followed by streptavidin-RPE (n=2). (*C,D*) Representative SPR sensorgrams showing binding to (*C*) HLA-DQ2.5:DQ2.5-glia-ω1 (n=2) and (*D*) HLA-DQ2.2:DQ2.5-glia-α1a (n=1) after capture of pMHC on sensor chips and injection of scFv clones as indicated. (*E*) SPR binding analysis of the HLA-DQ conformational-specific mAb SPV-L3 to evaluate the conformational integrity of HLA-DQ2.5:DQ2.5-glia-α1a, HLA-DQ2.5:DQ2.5-glia-ω1, HLA-DQ2.5:DQ2.5-glia-ω2, and HLA-DQ2.2:DQ2.5-glia-α1a as indicated after scFv binding experiments.

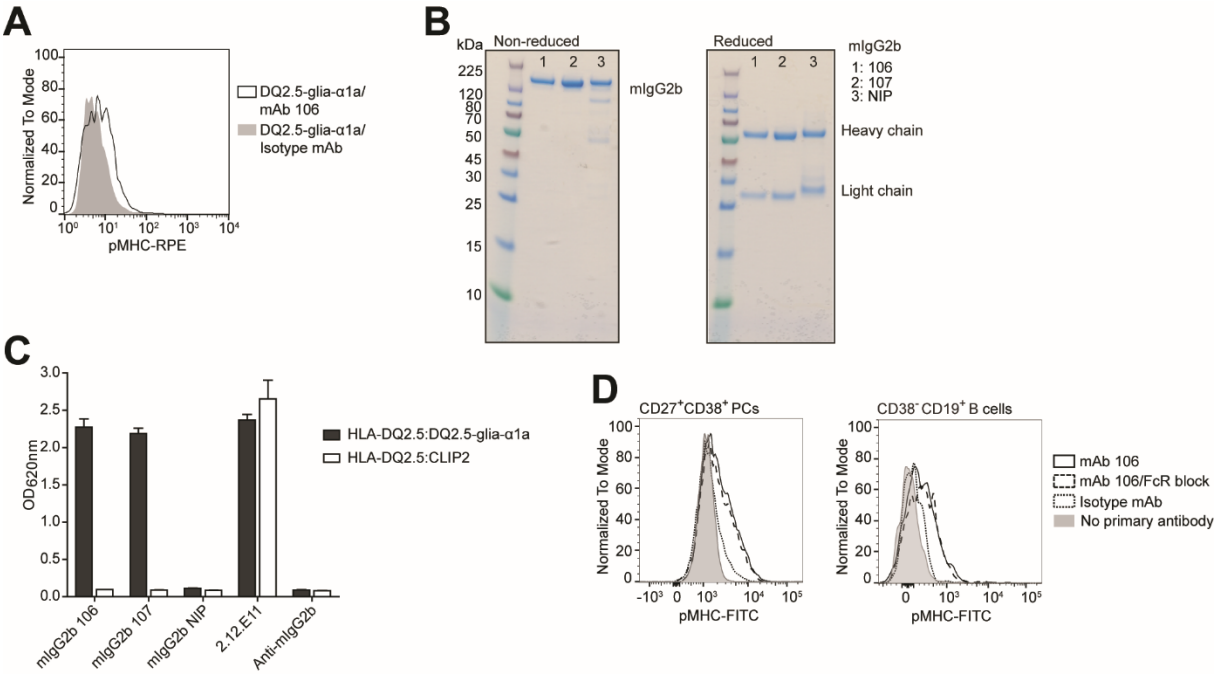

Supplementary Figure 3. Construction of mIgG2b mAbs and flow cytometric analysis of peptide-loaded cells and single-cell suspensions from celiac patient biopsies. (*A*) Monocyte-derived DCs were loaded with peptide and stained with hIgG1 mAb 106 or isotype control mAb before flow cytometric analysis (n=1). (*B*) SDS-PAGE gels of the mAbs 106 and 107 and isotype control mAb after reformatting to mIgG2b and purification from supernatants of transfected HEK293E cells. Full-length mIgG2b of approx. 150 kDa run under non-reducing conditions and separated heavy and light chains at approx. 50 kDa and 23 kDa run under reducing conditions are indicated. (*C*) Representative ELISA showing retained specificity of mIgG2b mAbs 106 and 107 after reformatting (n=2). mAb 2.12.E11 was included to control pMHC capture levels. (*D*) The figure is based on Fig. 3A showing detection of HLA-DQ2.5:DQ2.5-glia-α1a using mAb 106 with or without use of FcR block. Single-cell suspensions of intestinal biopsies from 3 patients all being HLA-DQ2.5^{+} with Marsh 3B/C were run in parallel.

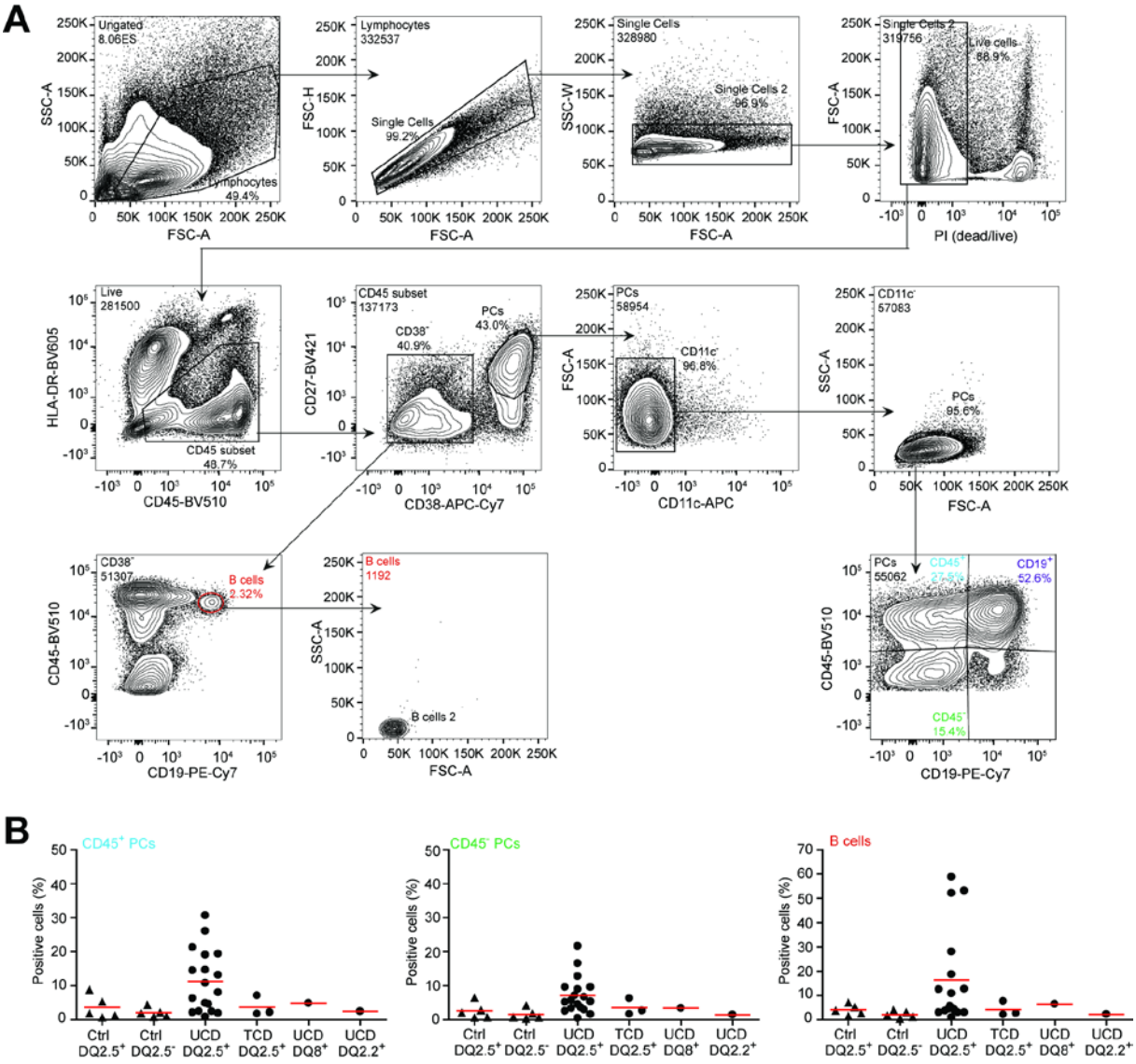

Supplementary Figure 4. Flow cytometric gating strategy and analysis of plasma cells and B cells presenting DQ2.5-glia-α1a peptide. Single-cell suspensions were prepared from intestinal biopsies, cells were stained with the indicated antibodies and immediately analyzed by flow cytometry. (*A*) Representative gating strategy for detection of gluten peptide presentation is shown. FSC-A, FSC-H and SSC-W were used to gate out doublet cells. (*B*) Stratification of the control patients among the CD45$^+$ plasma cells, CD45$^-$ plasma cells and B cells from Fig. 4B. Ctrl HLA-DQ2.5$^+$ (n=5), Ctrl HLA-DQ2.5$^-$ (n=5), UCD HLA-DQ2.5$^+$ (n=18), TCD HLA-DQ2.5$^+$ (n=3), UCD HLA-DQ8$^+$ (n=1), and UCD HLA-DQ2.2$^+$ (n=1). mIgG2b mAb 106 or 107 were used for detection and percent positive cells was determined relative to use of secondary antibody alone. Each data point represents an individual subject; non-celiac ctrl patients did not have mucosal alterations; red bars indicate mean percentage. (*A,B*) PCs, plasma cells.

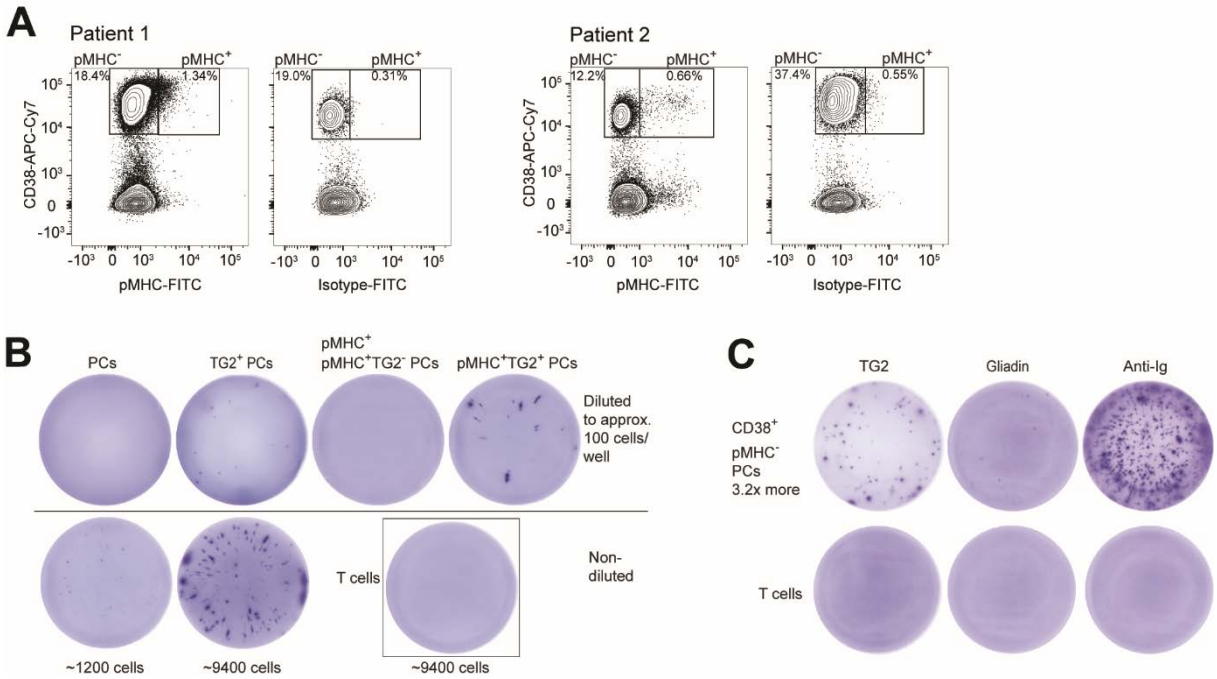

Supplementary Figure 5. FACS sorting of plasma cells for ELISPOT analyses. (*A*) pMHC$^+$ and pMHC$^-$ CD38$^+$ plasma cell populations (gated as large viable, CD38$^+$, CD11c$^-$, CD14$^-$, CD4$^-$ cells) that were assessed for IgA and IgM expression in Fig. 5A. Notably, the two populations were FACS sorted and used for the TG2 and gliadin ELISPOT shown in Fig. 5C and panel C of this figure. (*B*) Representative TG2-specific ELISPOT using the sorted plasma cell subsets as indicated (n=3). TG2-specific IgA autoantibodies were captured onto TG2-coated plates and detected using AP-conjugated anti-IgA Ab. T cells were used as negative control. (*C*) TG2 and gliadin ELISPOT. Upper panel; CD38$^+$ pMHC$^-$ plasma cells were used in approximately 3.2x higher numbers than as shown in Fig. 5C, resulting in increased spot frequency and also visible gliadin spots in this group. Lower panel; T cells were used as negative control. Derived from the same ELISPOT experiment as shown in Fig. 5C. (*B,C*) PCs, plasma cells.

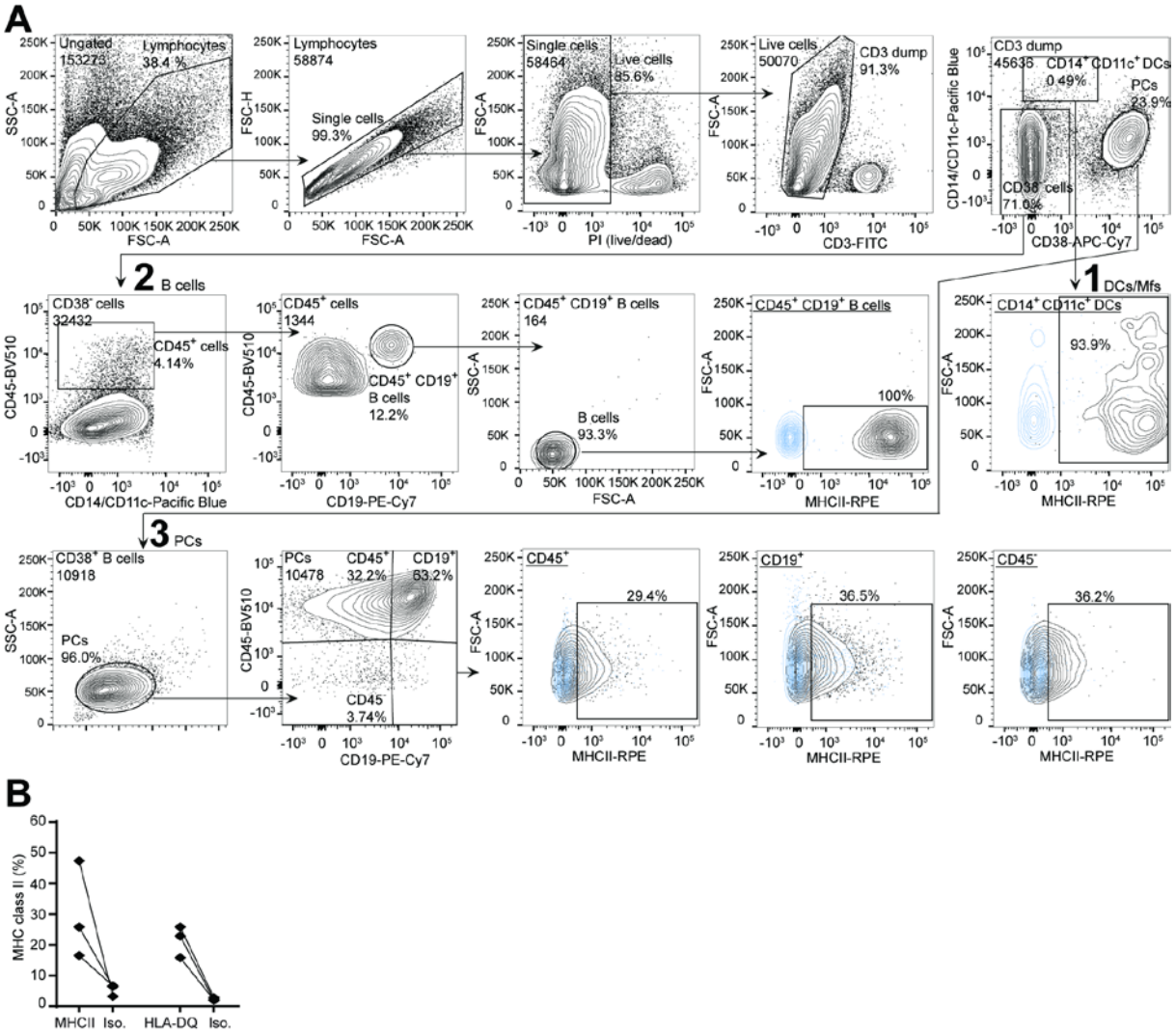

Supplementary Figure 6. (*A*) Gating strategy for detection of MHCII on APC subsets. Single-cell suspensions prepared from intestinal biopsies were stained with the indicated antibodies and immediately analyzed by flow cytometry. Representative gating strategy for detection of MHCII on bulk DCs and Mfs (1), B cells (2) and plasma cells (3) are shown. MHCII staining (black) is overlaid isotype control staining (blue). FSC-A and FSC-H were used to gate out doublet cells. PCs, plasma cells. (B) Percentage MHCII expression on bulk plasma cell subsets (large, viable, $CD19^{+/-}CD45^{+/-}CD38^{+}$) stained with either a pan-MHCII mAb or an HLA-DQ2 mAb. Material was obtained from patients undergoing Whipple procedure and confirmed to have a normal intestinal histology (n=3). Each data point represents an individual subject.

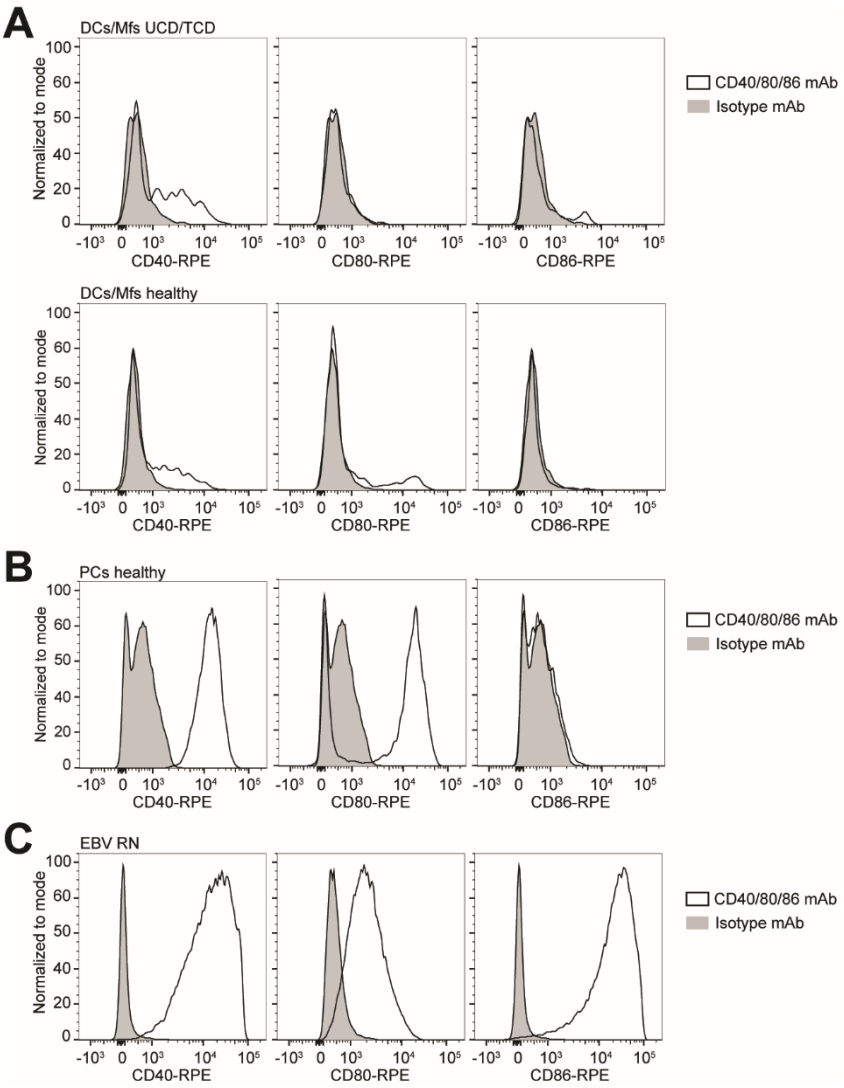

Supplementary Figure 7. (*A,B*) Representative staining for costimulatory markers CD40, CD80 and CD86. (*A*) Costimulatory marker expression profile on DCs/Mfs from UCD or TCD patients (n=4, 3 HLA-DQ2.5^{+} UCD patients with Marsh 3A/B and 1 TCD patient with Marsh 0) and from healthy, non-inflamed gut samples (n=3, all confirmed non-inflamed duodenum). (*B*) Expression profile on plasma cells from the same healthy, non-inflamed gut samples as above. PCs, plasma cells. (*C*) Staining of the EBV-B cell line RN (CD114) was included as a positive control.

Supplementary Table 1. Kinetics of the scFv-HLA-DQ2.5:DQ2.5-glia-α1a interaction.

	Single cycle kinetics[a]				Steady state[b]	
Clone	k_{on} ($M^{-1}s^{-1}$)	k_{off} (s^{-1})	K_D (M)	SE K_D (M)	K_D (M)	SE K_D (M)
scFv 106	$1.29x10^{5}$	0.01262	$9.79x10^{-8}$	$5.63x10^{-8}$	$1.42x10^{-7}$	$2.20x10^{-8}$
scFv 107	$2.89x10^{5}$	0.02151	$7.43x10^{-8}$	$7.44x10^{-8}$	$6.70x10^{-8}$	$1.30x10^{-8}$

[a] Kinetics were determined by fitting data to a 1:1 Langmuir binding model.

[b] Steady state K_D was derived from the single cycle kinetics runs.

Supplementary Table 2. Recombinant pMHCs and soluble peptides.

Recombinant pMHC	**Peptide amino acids**
HLA-DQ2.5:DQ2.5-glia-α1a[a]	QLQPFPQPELPY
HLA-DQ2.5:DQ2.5-glia-α1a-Q	QLQPFPQPQLPY
HLA-DQ2.5:DQ2.5-glia-α1a-pL7Q	QLQPFPQPEQPY
HLA-DQ2.5:DQ2.5-glia-α1a-pY9F	QLQPFPQPELPF
HLA-DQ2.5:DQ2.5-glia-α1a-Sα72I	QLQPFPQPELPY
HLA-DQ2.5:DQ2.5-glia-α2	PQPELPYPQPE
HLA-DQ2.5:DQ2.5-glia-ω1	QQPFPQPEQPFP
HLA-DQ2.5:DQ2.5-glia-ω2	FPQPEQPFPWQP
HLA-DQ2.5:DQ2.5-glia-γ1	PEQPQQSFPEQERP
HLA-DQ2.5:DQ2.5-glia-γ2	QGIIQPEQPAQL
HLA-DQ2.5:DQ2.5-glia-γ3	TEQPEQPYPQP
HLA-DQ2.5:DQ2.5-glia-γ4c	TEQPEQPFPQP
HLA-DQ2.5:CLIP2	MATPLLMQALPMGAL
Soluble peptides	**Peptide amino acids**
DQ2.5-glia-α1a	QLQPFPQPELPY
DQ2.5-glia-α2	PQPELPYPQPQL
33mer	LQLQPFPQPELPYPQPELPYPQPELPYPQPQPF

The 9mer core sequence constituting the T-cell epitope is underlined and all peptides are in their deamidated form unless otherwise specified (native=Q). Soluble, recombinant pMHCs were generated as previously described[1]

[a] Or HLA-DQ2.2.

Supplementary Table 3. Antibodies used for ELISA.

Antigen	Conjugate	Clone	Supplier	Dilution
NeutrAvidin	-	-	Avidity	10 µg/ml
M13	HRP	Monoclonal	GE Healthcare	1:5000
His-tag	HRP	AD1.1.10	AbD Serotech	1:5000
Human IgG Fc	AP	Polyclonal	Sigma	1:2000
HLA-DQ	-	2.12.E11	Diatech[2]	1 µg/ml
Mouse IgG Fc	AP	Polyclonal	Sigma	1:2000

Normalized amounts of soluble, recombinant pMHC were captured onto the NeutrAvidin coated plates, before addition of phage/periplasmic fractions/0.5 µg/ml hIgG1. Samples were detected with anti-M13-HRP/anti-His-tag-HRP/anti-human IgG Fc-AP, respectively; mAb 2.12.E11 detected using anti-mouse IgG Fc-AP; 0.1 µg/ml hIgG1 was pre-incubated 30 min with non-biotinylated pMHC/peptides 2-fold diluted from 1 µM for competition assays (peptides specified in Supplementary Table 2). PBS supplemented with 4% (w/v) non-fat skim milk powder was used to block plates, and PBS supplemented with 0.05% (v/v) Tween-20 was used as buffer for dilution of samples and for washing the plates between each layer.

Supplementary Table 4. Antibodies used for flow cytometry.

Antigen	Conjugate	Clone	Supplier	Dilution
Staining of A20 B cells and peptide-loaded monocyte-derived DCs[c]				
hIgG1 106/107	-	106, 107	In-house	10 µg/ml
hIgG (F(ab')2)[a]	Biotin	Polyclonal	Southern Biotech	2 µg/ml
HLA-DQ2[a]	Biotin	2.12.E.11	Diatech[2]	10 µg/ml
Isotype control	Biotin	15H6	Southern Biotech	10 µg/ml
Staining of pMHC on DC, Mfs, plasma cells and B cells[d]				
mIgG2b 106/107	-	106, 107	In-house	10 µg/ml
Isotype control	-	NIP, MPC-11	In-house, Sigma	10 µg/ml
mIgG2b	FITC	Polyclonal	Southern Biotech	1 µg/ml
CD3	APC	OKT3	eBioscience	1:20
CD11c	APC	S-HCl-3	BD Biosciences	1:20
CD14	APC	HCD14	Biolegend	1:20
CD14	APC-Cy7	HCD14	Biolegend	1:20
HLA-DR	BV605	L243	Biolegend	1:20
CD45	BV510	H130	Biolegend	1:20
CD19	PE-Cy7	HIB19	Biolegend	1:20
CD38	APC-Cy7	HIT2	Biolegend	1:20
CD27	BV421	O323	Biolegend	1:20
Staining of MHCII on DC, Mfs, plasma cells and B cells[d]				
HLA-DP/DR/DQ/Dx	-	CR3/43	Santa Cruz Biotechnology	10 µg/ml
Isotype ctrl.	-	MOPC-21	BD Pharmingen	10 µg/ml
mIgG1	PE	A85-1	BD Biosciences	1 µg/ml
HLA-DQ	-	SPV-L3	Diatech	10 µg/ml
Isotype ctrl.	-	HOPC-1	Southern Biotech	10 µg/ml
mIgG2a	PE	RMG2a-62	Biolegend	1 µg/ml
CD3	FITC	OKT3	Biolegend	1:50
CD11c	BV450	B-Ly6	BD Horizon	1:20
CD14	Pacific Blue	M5E2	BD Pharmingen	1:20
CD45	BV510	H130	Biolegend	1:20
CD19	PE-Cy7	HIB19	Biolegend	1:20
CD38	APC-Cy7	HIT2	Biolegend	1:20
TG2 multimers[b]	APC	-	In-house	
Staining of co-stimulatory molecules[d]				
CD3	FITC	OKT3	Biolegend	1:50
CD11c	APC	S-HCl-3	BD Biosciences	1:20
CD14	APC	HCD14	Biolegend	1:20
CD45	BV510	H130	Biolegend	1:20
CD19	PE-Cy7	HIB19	Biolegend	1:20
CD38	APC-Cy7	HIT2	Biolegend	1:20
CD27	BV421	O323	Biolegend	1:20
CD40	PE	HI40a	ImmunoTools	1:20
CD80	PE	MEM-233	SeroTech	1:20
CD86	PE	2331 (FUN-1)	BD Pharmingen	1:20
Isotype ctrl.	PE	P3.6.2.8.1	eBioscience	1:20

1x PBS supplemented with 5% FCS and 0.1% NaN_3 was used as staining buffer and all stainings were performed on ice and with centrifugations at 4°C.

[a] Detected with streptavidin RPE (Invitrogen).

[b] Prepared by preincubation of biotinylated TG2 with Strep-tactin-APC (iba solutions) as described[3].

[c] Dead cells were excluded using 7-AAD and samples were immediate analysis on FACSCalibur (BD).

[d] Propidium iodide exclusion of dead cells and human FcR Blocking Reagent (Miltenyi Biotec) was included. Cells were immediately acquired on LSR Fortessa cytometer (BD).

Supplementary Table 5. Antibodies used for FACS sorting.

Antigen	Conjugate	Clone	Supplier	Dilution
Sorting of plasma cells, panel 1				
hIgG1 106	Alexa-488	106	In-house	10 µg/ml
hIgG1 RSV	Alexa-488	RSV	In-house	10 µg/ml
CD4	Pacific Blue	SK3	Biolegend	1:33
CD8	Pacific Blue	SK1	Biolegend	1:33
CD14	Pacific Blue	M5E2	Biolegend	1:33
CD11c	BV450	B-Ly6	BD Horizon	1:33
CD27	PE-Cy7	LG.7F9	eBioscience	1:500
IgA	PE	Polyclonal	Southern Biotech	1:2000
TG2 multimers[a]	APC	-	In-house	
Sorting of plasma cells, panel 2				
mIgG2b 107	-	107	In-house	10 µg/ml
Isotype control	-	NIP, OMV	In-house[4]	10 µg/ml
mIgG2b	FITC	Polyclonal	Southern Biotech	1 µg/ml
CD4	Pacific Blue	SK3	Biolegend	1:20
CD14	Pacific Blue	M5E2	Biolegend	1:20
CD11c	BV450	B-Ly6	BD Horizon	1:20
CD38	APC-Cy7	HIT2	Biolegend	1:20
IgA	APC	REA1014	MACS	1:20
IgM	PE	SA-DA4	eBioscience	1:20

1x PBS supplemented with 5% FCS and 0.1% NaN_3 was used as staining buffer and all stainings were performed on ice and with centrifugations at 4°C. Samples were sorted on FACSAriaII (BD) with a 100 µM nozzle.

[a] Prepared by preincubation of biotinylated TG2 with Strep-tactin-APC (iba solutions) as described[3].

References

1. Quarsten H, McAdam SN, Jensen T, et al. Staining of celiac disease-relevant T cells by peptide-DQ2 multimers. J Immunol 2001;167:4861-8.
2. Viken HD, Paulsen G, Sollid LM, et al. Characterization of an HLA-DQ2-specific monoclonal antibody. Influence of amino acid substitutions in DQ beta 1*0202. Hum Immunol 1995;42:319-27.
3. Snir O, Mesin L, Gidoni M, et al. Analysis of celiac disease autoreactive gut plasma cells and their corresponding memory compartment in peripheral blood using high-throughput sequencing. J Immunol 2015;194:5703-12.
4. Høydahl LS, Nilssen NR, Gunnarsen KS, et al. Multivalent pIX phage display selects for distinct and improved antibody properties. Sci Rep 2016;6:39066.